

# Structural Performance of Spoke Wheel Roof Systems

By

**Harry Kim**

Bachelor of Engineering in Civil Engineering

The Cooper Union for the Advancement of Science and Art, 2016

Submitted to the Department of Civil and Environmental Engineering in Partial Fulfillment of  
the Requirements for the Degree of

**MASTER OF ENGINEERING IN CIVIL AND ENVIRONMENTAL ENGINEERING**

at the

**MASSACHUSETTS INSTITUTE OF TECHNOLOGY**

June 2017

©2017 Harry Kim. All rights reserved.

The author hereby grants to MIT permission to reproduce and to distribute publicly paper and electronic copies of this thesis document in whole or in part in any medium now known or hereafter created.

**Signature redacted**

Signature of Author: \_\_\_\_\_

Department of Civil and Environmental Engineering

May 19, 2017

**Signature redacted**

Certified by: \_\_\_\_\_

Gordana Héring

Postdoctoral Lecturer of Civil and Environmental Engineering

Thesis Supervisor

**Signature redacted**

Certified by: \_\_\_\_\_

John A. Ochsendorf

Class of 1942 Professor of Civil and Environmental Engineering and Architecture

Thesis Supervisor

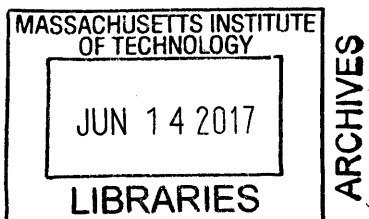
**Signature redacted**

Accepted by: \_\_\_\_\_

Jesse Kröll

Professor of Civil and Environmental Engineering

Chair, Graduate Program Committee





# **Structural Performance of Spoke Wheel Roof Systems**

By

Harry Kim

Submitted to the Department of Civil and Environmental Engineering

on May 19, 2017 in Partial Fulfillment of the

Requirements for the Degree of Master of Engineering in

Civil and Environmental Engineering

## **ABSTRACT**

A spoke wheel roof system consists of tension rings, compression rings, and radial spokes and resists loads mainly through axial forces. Due to its light weight and ability to achieve a column-free, long span, it has been a popular solution to structures such as stadia since its first use in 1960s. However, there has been lack of information on the performance of a spoke wheel roof system depending on its geometry.

This thesis explores the history and general behaviors of a spoke wheel roof system. A representative model is created and tested in Rhino-Grasshopper-Karamba, and the geometric variations to the structure and their influence are evaluated. Configuration of the rings, inner and outer ring radii, aspect ratios of the rings, spoke spacing and slope are chosen to be variables, and load path is used as an evaluation criterion for structural performance or efficiency.

Results show that the choice between different ring configurations depends on architectural needs and climate conditions. Assuming that minimal load path implies high structural performance, roof span and size are inversely related to the structural performance. They have a greater influence than the aspect ratios of the rings. Smaller spacing and larger slope of the spokes lead to a more efficient structure.

Thesis Supervisor: Gordana Herning

Title: Postdoctoral Lecturer of Civil and Environmental Engineering

Thesis Supervisor: John A. Ochsendorf

Title: Class of 1942 Professor of Civil and Environmental Engineering and Architecture

This page is intentionally left blank.

## Acknowledgments

This thesis and my completion of the program may not have been possible without immense support from so many individuals I am thankful to have around.

First, I would like to express my sincere gratitude to my thesis advisor, Gordana Herning, for her tremendous support and brilliant comments throughout the research process. From the formation of the research question to the completion of the thesis, she was always patient and willing to spend hours to answer my questions and give me better insights on the challenges I faced. Her constant encouragement and caring helped me go through challenges, and chit-chat with her over a chocolate bar was the biggest refreshment when I was stressed out from the thesis. I am thankful to have had her as my thesis advisor and inspiration.

I would like to thank my parents for their unconditional love and support, and being the reason for and driving force of my life. Their tremendous emotional support helped me get invaluable educational opportunities, try new things, and stay positive all the time. Thanks to them being my parents, my world is full of happiness and motivation. Words are never enough to express how much I am thankful for them and love them.

I would like to thank the other faculty and staff members of the MIT Civil and Environmental Engineering, including John Ochsendorf and Caitlin Mueller, for giving me an opportunity to study at MIT, and Robert Silman at Harvard University, for teaching me valuable structural engineering concepts.

I would like to thank all my friends that I met at or before MIT, for making my life much more enjoyable. My special gratitude goes to the M.Eng. class of 2017 and Ae-woo-hoe, for being inspirational and always having made me laugh for the past 9 months.

This page is intentionally left blank.

# Table of Contents

ABSTRACT.....	3
Acknowledgments.....	5
Table of Contents.....	7
List of Figures.....	9
List of Tables.....	11
1. Introduction.....	12
A. Motivation.....	12
B. Background.....	13
a) Spoke Wheel System.....	13
b) Spoke Wheel Roof System.....	13
i) Non-pre-tensioned spokes.....	14
ii) Pre-tensioned spokes.....	15
iii) Non-circular shape.....	17
iv) Efficient Structure.....	18
c) Literature Review.....	19
d) Precedents.....	21
2. Methodology and Model.....	31
A. Methodology.....	31
a) Platform.....	31
b) Analysis Procedure.....	31
i) Effect of Pre-tension.....	31
ii) Grasshopper-Karamaba.....	34
B. Model.....	35
a) Reference Project.....	35
b) Ring Configuration.....	37
c) Material and Section Properties.....	38
d) Connection.....	39
e) Supports.....	39
f) Location.....	40
g) Building Code and Loads.....	41
i) Load Cases.....	41

ii) Dead Load .....	42
iii) Wind Load.....	43
iv) Snow Load.....	46
v) Live Load.....	47
vi) Rain Load .....	47
vii) Seismic Load .....	47
C. Variables and Objective .....	48
a) Variables .....	48
i) Ring Configuration.....	48
ii) Radii of the Inner and Outer Rings.....	48
iii) Aspect Ratio .....	49
iv) Spoke Spacing and Slope .....	49
b) Evaluation Criterion .....	51
3. Results.....	54
A. Change of Inner and Outer Ring Radii .....	54
B. Configuration .....	57
C. Aspect Ratio.....	58
D. Spoke Spacing and Slope.....	61
4. Conclusion .....	63
References.....	65



# List of Figures

Figure 1. Spoke wheel roof configurations: (a) post-tensioned, (b) pre-tensioned with two inner rings + one outer ring, and (c) pre-tensioned with one inner ring + two outer rings (Krishna, 1990) ..... 13

Figure 2. Force distribution within a non-pre-tensioned spoke wheel roof with double inner rings and one outer ring (Boom, 2012) ..... 14

Figure 3. Force distribution within a pre-tensioned spoke wheel roof: (a) double inner rings and single outer ring and (b) single inner ring and double outer rings (Boom, 2012) ..... 15

Figure 4. Cable truss action in a pre-tensioned roof system: (a) normal forces in the structural elements and (b) development of radial pre-stress (Bergermann and Göppert, 2000) ..... 15

Figure 5. Variation of the inner ring and the corresponding amount of materials required for Pusan Dome in South Korea (Bergermann and Göppert, 2000) ..... 16

Figure 6. Evolution of a spoke wheel roof system (Bergermann and Göppert, 2000) ..... 17

Figure 7. Ring and truss elements configurations in the thesis of Boom (2012): (a) “Variant 1” with members connecting the curved corner of the outer ring and the straight part of the inner ring, (b) “Variant 2” without such connecting members ..... 19

Figure 8. Utica Memorial Roof (Allen and Zalewski, 2010) ..... 21

Figure 9. Roof Structure of the Madison Square Garden (Building with steel, 1968) ..... 21

Figure 10-a. Utica Memorial Auditorium (Source: Utica Memorial Auditorium [Photograph], Retrieved from <http://www.columbia.edu/cu/gsap/BT/BSI/TENSEGRI/tensegri.html>) ..... 22

Figure 10-b. Palasport di Genova (Source: Cepolina, F. (Photographer). (2014). Genoa Palasport ceiling net [Photograph], Retrieved from <http://www.cepolina.com/Genoa-Palasport-ceiling-net.html>) ..... 22

Figure 10-c. Madison Square Garden (Source: Madison Square Garden under Construction [Photograph]. (1967). Retrieved from <https://historiasdenuevayork.es/tag/madison-square-garden-under-construction/>)23

Figure 10-d. Plaza de Toros of Zaragoza (Source: schlaich bergermann partner. (Photographer). Bull ring roof Zaragoza (Plaza de Toros) [Photograph], Retrieved from <http://www.sbp.de/en/project/bull-ring-roof-zaragoza-plaza-de-toros/>) ..... 23

Figure 10-e. Mercedes-Benz Arena (Source: Storck, M. (Photographer). Gottlieb-Daimler-Stadium [Photograph], Retrieved from <http://www.sbp.de/en/project/gottlieb-daimler-stadium/>) ..... 23

Figure 10-f. Gerry Weber Stadium (Bergermann and Göppert, 2000) ..... 24

Figure 10-g. De Kuip (Boom, 2012) ..... 24

Figure 10-h. Bukit Jalil National Stadium (Source: NSC Roof Outdoor Stadium Kuala Lumpur [Photograph], Retrieved from <http://www.sbp.de/en/project/nsc-roof-outdoor-stadium-kuala-lumpur/>) .. 24

Figure 10-i. Estadio Olimpico (Source: Olympic Stadium Seville [Photograph], Retrieved from <http://www.sbp.de/en/project/olympic-stadium-seville/>) ..... 25

Figure 10-j. Volkspark Stadium Hamburg (Source: Coddou, R. (Photographer). Volkspark Stadium Hamburg [Photograph], Retrieved from <a href="http://www.sbp.de/en/project/volkspark-stadium-hamburg/">http://www.sbp.de/en/project/volkspark-stadium-hamburg/</a> ) ...	25
Figure 10-k. Pusan Sports Dome (Source: schlaich bergemann partner. (Photographer). Pusan Dome [Photograph], Retrieved from <a href="http://www.sbp.de/en/project/pusan-dome/">http://www.sbp.de/en/project/pusan-dome/</a> ) .....	26
Figure 10-l. Volkswagen Arena (Source: Volkswagen-Arena-Wolfsburg [Photograph], Retrieved from <a href="http://www.europlan-online.de/volkswagen-arena/stadion-109.html">http://www.europlan-online.de/volkswagen-arena/stadion-109.html</a> ) .....	26
Figure 10-m. National Athletics Stadium Abuja (Source: National Athletics Stadium Abuja [Photograph], Retrieved from <a href="http://www.sbp.de/en/project/national-athletics-stadium-abuja/">http://www.sbp.de/en/project/national-athletics-stadium-abuja/</a> ) .....	26
Figure 10-n. Commerzbank Arena (Source: fantastic new media gmbh. (Photographer). Commerzbank-Arena Frankfurt (former Waldstadion) [Photograph], Retrieved from <a href="http://www.sbp.de/en/project/commerzbank-arena-frankfurt-former-waldstadion/">http://www.sbp.de/en/project/commerzbank-arena-frankfurt-former-waldstadion/</a> ) .....	27
Figure 10-o. Bay Arena Leverkusen (Source: Bayer 04 Leverkusen Fußball GmbH. (Photographer). BayArena Leverkusen [Photograph], Retrieved from <a href="http://www.sbp.de/en/project/bayarena-leverkusen/">http://www.sbp.de/en/project/bayarena-leverkusen/</a> ) .....	27
Figure 10-p. Jawaharlal Nehru Stadium (Source: JNS Jawaharlal Nehru Stadium [Photograph], Retrieved from <a href="http://www.sbp.de/en/project/jns-jawaharlal-nehru-stadium/">http://www.sbp.de/en/project/jns-jawaharlal-nehru-stadium/</a> ) .....	27
Figure 10-q. Moses Mabhida Stadium (Source: schlaich bergemann partner. (Photographer). Moses Mabhida Stadium [Photograph], Retrieved from <a href="http://www.sbp.de/en/project/moses-mabhida-stadium/">http://www.sbp.de/en/project/moses-mabhida-stadium/</a> ) .....	28
Figure 10-r. The Forum (Source: INGLEWOOD - The Forum [Photograph], Retrieved from <a href="http://www.skyscrapercity.com/showthread.php?p=110702389">http://www.skyscrapercity.com/showthread.php?p=110702389</a> ) .....	28
Figure 10-s. Maracanã Stadium (Source: Bredt, M. (Photographer). Stadium Maracanã (Estádio Jornalista Mário Filho) [Photograph], Retrieved from <a href="http://www.sbp.de/en/project/stadium-maracana-estadio-jornalista-mario-filho/">http://www.sbp.de/en/project/stadium-maracana-estadio-jornalista-mario-filho/</a> ) .....	28
Figure 10-t. Stadium FK Krasnodar (Source: Bredt, M. (Photographer). Stadium FK Krasnodar [Photograph], Retrieved from <a href="http://www.sbp.de/en/project/stadium-fk-krasnodar/">http://www.sbp.de/en/project/stadium-fk-krasnodar/</a> ) .....	29
Figure 11. Pre-tensioned truss element (Ghisbain, 2013) .....	32
Figure 12. Analysis procedure considering pre-tension .....	33
Figure 13. Modify Element and AnalyzeThII components in Grasshopper-Karamba .....	35
Figure 14. Drawings of the Zaragoza Arena roof: (a) plan and (b) elevation views .....	36
Figure 15. Membrane position for the two configurations: (a) Configuration 1 and (b) Configuration 2 ..	37
Figure 16. Spacing between the vertical struts or ties: (a) Configuration 1 and (b) Configuration 2 .....	38
Figure 17. Support conditions for the outer ring, where circles and triangles show roller and pin supports, respectively .....	40
Figure 18. Annual dry bulb temperature in Zaragoza, Spain and New York City, USA .....	41
Figure 19. Wind load critical conditions: (a) Wind Load Case 1 (W1) and (b) Wind Load Case 2 (W2) .	45

Figure 20. Wind load application for (a) Configuration 1 and (2) Configuration 2 .....	46
Figure 21. Snow load application for (a) Configuration 1 and (2) Configuration 2 .....	47
Figure 22. Structural weight comparison: cantilevered vs. spoke wheel structure (Masubuchi, 2013) .....	48
Figure 23. Load Path Factor for circular roof Configurations C1 and C2 when inner (r1) and outer (r2) radii are varied.....	55
Figure 24. Change in the total length factor with respect to the roof span, when either inner (r1) or outer (r2) radius is varied .....	56
Figure 25. Change in the total roof coverage area with respect to the roof span when either inner (r1) or outer (r2) radius is varied .....	56
Figure 26. Normalized total element lengths and normalized load path values for Configurations 1 and 2..	57
Figure 27. Load path factor and roof span change depending on the aspect ratio change of the inner or outer rings (R(r1) or R(r2)) and configurations 1 (C1) or 2 (C2) .....	59
Figure 28. Load Path Factor when both the inner and outer rings have the same aspect ratio R .....	60
Figure 29. Load Path Factor when spoke spacing ( $\alpha$ ) is varied.....	61
Figure 30. Load Path Factor when spoke slope ( $\theta$ ) is varied .....	62

## List of Tables

Table 1. Material properties for the model .....	39
Table 2. Wind load for windward and leeward sides .....	45
Table 3. Geometric variables for the design .....	50
Table 4. Sample calculation of load path factors .....	55
Table 5. Base variable settings .....	55
Table 6. Different approaches of varying the aspect ratio .....	59

# 1. Introduction

## A. Motivation

A spoke wheel roof structure has been widely used since its first introduction in the 1960s and its great improvement with double-ring and pre-tension systems in the 1980s. With the efficient load transfer mainly with axial members, a spoke wheel roof system uses less materials and is effective in covering a large span without inner columns. Due to its light weight and clear long span, it has been used mostly for stadia. It has been a popular solution especially to existing structures, since it imposes relatively small dead load onto the existing structure and foundation, and does not need special supports to be installed.

Similar to a spoke wheel used for bicycles, a spoke wheel roof structure consists of tension ring(s), compression ring(s), and radial spokes. Over the past decades, its geometry has been varied to meet the architectural needs and geometric limitations. First, the structure had non-pre-tensioned spokes with a single layer of tension and compression rings. Then double tension or compression rings and pre-tensioned spokes were introduced to make the structure stiffer and more efficient and have an opening at its center. Oval-shaped rims were also introduced. Along with other variables including spoke and membrane roof covering properties, support types, and connection conditions, a spoke wheel roof system has been modified to be applied to each project.

However, the information on the influence of each variable to the overall performance of the structure is scarce. The design of a spoke wheel roof structure has been case-specific, and there has been lack of information on how the design decisions affect the general behavior of the system. This thesis aims to find out how each variable influences the performance of a spoke wheel roof system. In order to narrow down the scope of the thesis, the variables are limited to geometric ones.

## **B. Background**

### **a) Spoke Wheel System**

Invention of a wheel is considered as one of the greatest feats in the human history, as it has enabled transportation of loads with minimal energy. Whereas the early versions of a wheel around 3000 BC were heavy with thick and rigid wooden planks, introduction of spokes between the hub and the rim of the wheel around 2000 BC led to a significant improvement of its performance. The wheel became much lighter through the transformation of planks into spokes. It improved greatly again in the early 1800s, an English engineer George Cayley introduced “pre-tensioned” spokes, in which pre-tension prevents the spokes from becoming slack and collapsing when applied loads increase compression in them. As long as the pre-tensioned spokes are in tension, they are rigid (Brandt, 2003).

For a bicycle wheel, spoke tension is the primary static load. Pre-tensioning force in the spokes and compressive force in the rim are dependent on each other. When radial load from the weight of a cyclist is applied, it is applied at the hub and displaces the rim. The portion of the rim that has contact with the ground under the load is called the load-affected zone, and the spokes within that zone experience change of stress (Brandt, 2003).

The strength of a bicycle wheel increases when there is more pre-tension, which can prevent spoke failure under larger compressive force. It is also improved by increasing the rim cross-section for higher bending and torsional rigidity, lengthening the load-affected zone and distributing loads over more spokes, or using thinner and more elastic spokes which can absorb more energy.

Stiffness is defined as the ratio of load to displacement. The radial stiffness, the measure of the force to deflect the rim radially, is enhanced when the number and thickness of spokes increase. Stiffer rims and shorter spokes also contribute to greater radial stiffness. Meanwhile, the transverse stiffness, which resists sideways deflection of the rim, is increased by using larger flange spacing, bigger rim strength, and more or thicker spokes.

### **b) Spoke Wheel Roof System**

A spoke-wheel roof system, or a bicycle wheel roof system, is defined as a system which consists of tension ring(s), compression ring(s), and radial spokes. In the system, applied loads are primarily supported through axial forces.

Starting from the 1960s, a spoke wheel system has been applied for the design of roof structures. Early design of spoke wheel roof systems made use of cable trusses, which were stiffened or post-

tensioned afterwards by additional loads imposed on them, which were sometimes provided by concrete decks above. In the 1980s, central openings and pre-tensioned cables started to be used. Figure 1 illustrates the post-tensioned and pre-tensioned spoke wheel roof structures. Pre-tensioning is used to give additional tensile stress to a structural member, especially to increase the stiffness of a flexible member under all possible loads. In a spoke wheel roof, a compression ring acts as a pair of horizontal arches. Two layers of radial spokes primarily take downward and upward loads such as gravity and wind uplift forces.

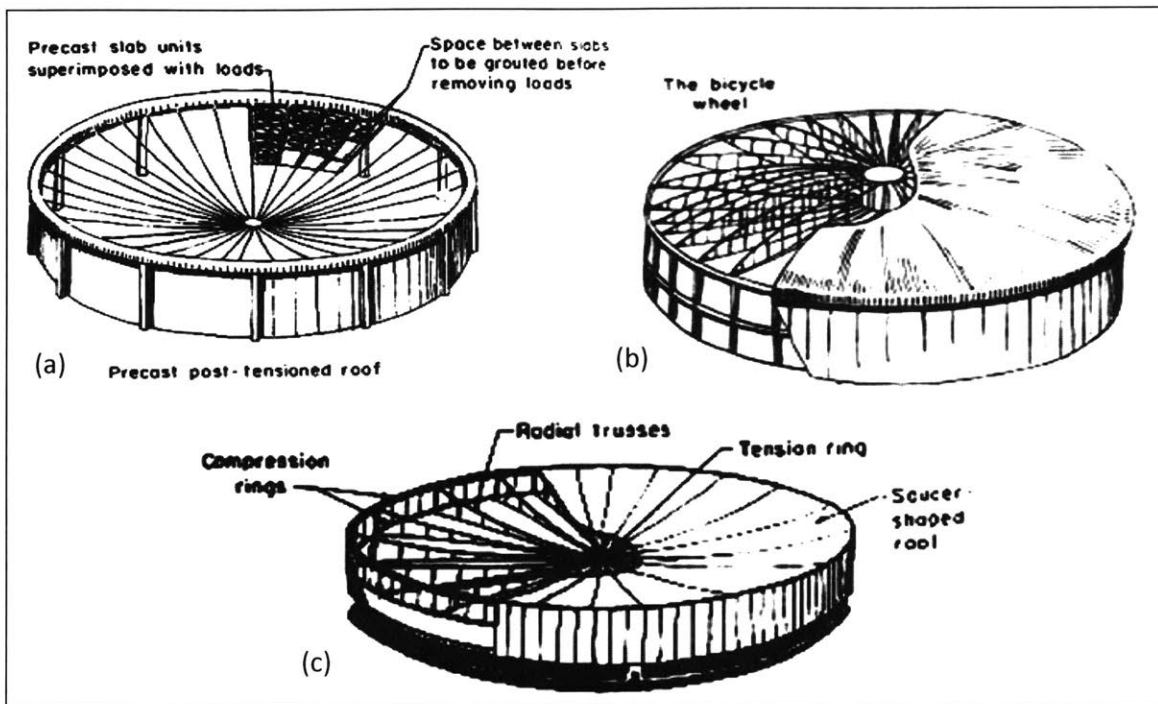


Figure 1. Spoke wheel roof configurations: (a) post-tensioned, (b) pre-tensioned with two inner rings + one outer ring, and (c) pre-tensioned with one inner ring + two outer rings (Krishna, 1990)

Compared to a bicycle wheel which is supported at its center hub, a spoke wheel roof is supported at its outer rim. The rim of a bicycle wheel can translate either radially or laterally. On the other hand, a spoke wheel roof is fixed perpendicular to the ground, while its translation in radial direction is partially allowed in order to support transverse or lateral load through axial forces in the structural elements.

Spoke wheel roof systems have evolved with the following characteristics.

#### i) Non-pre-tensioned spokes

Even in the case where the spokes are not pre-tensioned, a spoke wheel roof still functions as an efficient structure (Allen E. & Zalewski, W, 2010). The early examples of non-pre-tensioned spoke wheel

roofs include the Madison Square Garden that was built in New York, USA, in 1958, which is described in details in Section 1.B.d.

Because the spokes are not pre-tensioned, some of them are subjected to compression, which requires them to be truss members but not cables. For a system with two inner rings and one outer ring, the upper spokes become compression members. The lower inner ring is also under compression, being a compression ring, as shown in Figure 2. As there are more compression members, the structure becomes more sensitive to buckling and is less ideal than a pre-tensioned structure. The location of the rings alone, either on the inner or outer side, does not decide whether they transfer force in tension or compression; it is the combination of the location and pre-tensioning that direct the force flow in a way preferred by the designer.

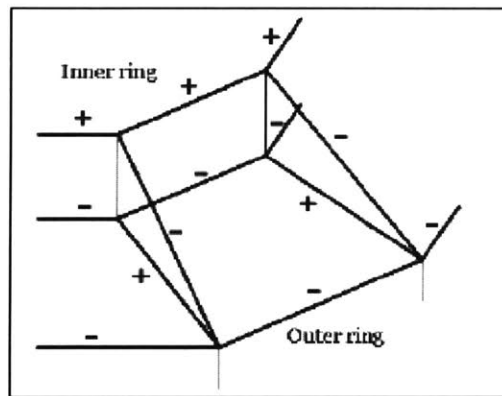


Figure 2. Force distribution within a non-pre-tensioned spoke wheel roof with double inner rings and one outer ring (Boom, 2012)

### ii) Pre-tensioned spokes

As pre-tensioned spokes led to a great improvement in a bicycle spoke wheel, pre-tensioned radial spoke members also brought innovation to a spoke wheel roof structure. Pre-tensioning the radial spokes could stabilize the structure without imposing additional dead load such as concrete deck to stiffen it, and having an opening at the center of the roof was enabled. Two configurations are possible by using the pre-tensioned members: (1) the one with double inner tension rings and single outer compression ring, and (2) the other with single inner tension ring and double outer compression rings. Factors such as the overall shape of the roof and geometric limitations lead to the decision to use one configuration over the other.

When the spokes are pre-tensioned, the force flow within the structure changes. The pre-tensioned members are “directed” to take loads in tension, counter-balancing any compressive force that may be induced in them. The force generated in the inner and outer rings by pre-tensioning is resolved through

either tension or compression. With the pre-tensioned spokes, the inner rings are pre-tensioned if needed and become tension rings, and only the outer rings become compression members as shown in Figure 3.

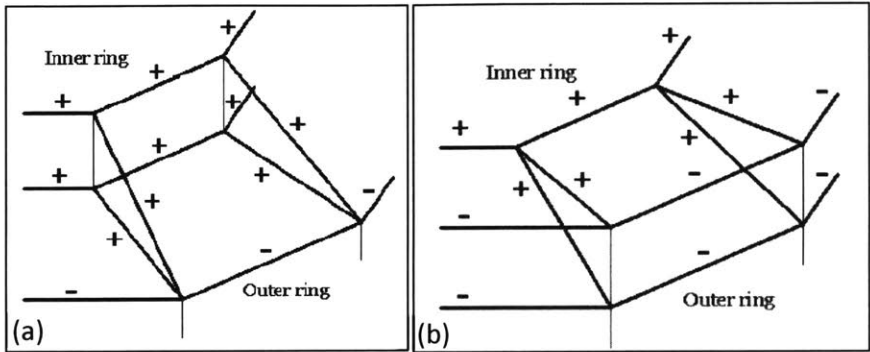


Figure 3. Force distribution within a pre-tensioned spoke wheel roof: (a) double inner rings and single outer ring and (b) single inner ring and double outer rings (Boom, 2012)

Bergermann and Göppert (2000) showed the force distribution in a spoke wheel structure with pre-tensioned radial spokes, double compression rings and one tension ring through graphical force diagrams as in Figure 4-(a) and (b). Given an external load of  $P$ , compression force  $D$  and tension force  $V$  are generated in the lower and upper cables, respectively. The compression force  $D$  in the lower cable can be fully eliminated when the pre-tension  $V_u$  is provided, which is bigger than  $D$ . Due to pre-tension  $V_u$  and  $V_o$  in the lower and upper cables, the resultant horizontal force  $V$  is generated.  $V$  can be relieved through tension force in the inner tension ring, as shown in the Figure 4-(b).

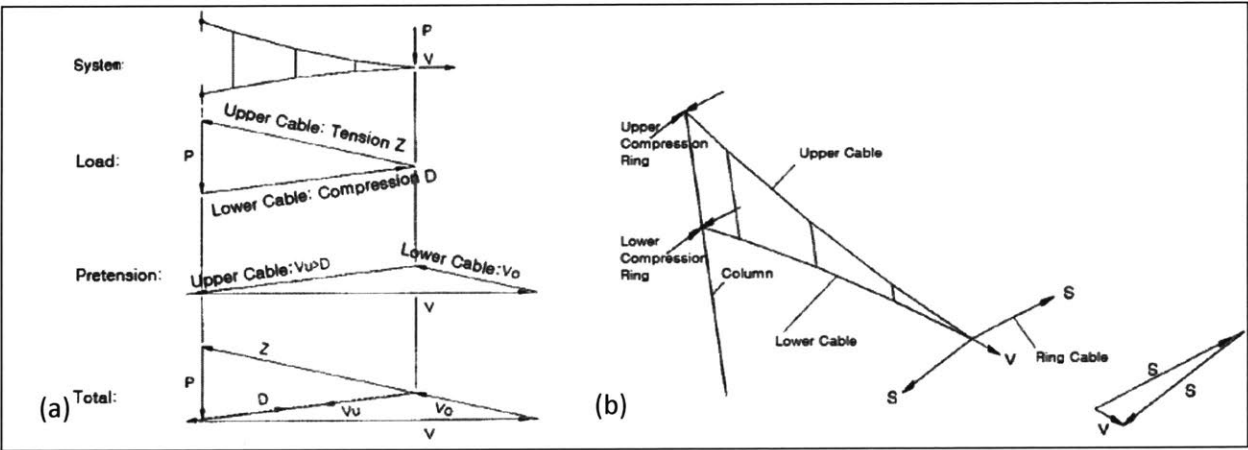


Figure 4. Cable truss action in a pre-tensioned roof system: (a) normal forces in the structural elements and (b) development of radial pre-stress (Bergermann and Göppert, 2000)



### iii) Non-circular shape

Because a spoke wheel roof system has been widely used as a stadium roof, modifications to its overall geometry have been made to satisfy the architectural and geometric limitation. One of them was to make the roof oval, as some sports fields were in rectangular shapes, requiring the stadium to accommodate this geometry.

The oval shape does not result in additional problems such as the generation of bending stress in the rims, as long as the centers of the inner and outer rings coincide, and the rings are in the same shape (Bergermann and Göppert, 2000).

When the shapes of the inner and outer rings differ from each other, the efficiency of the design may decrease. Figure 5 shows the relationship between the inner ring geometry and the total amount of materials required for the Pusan Dome in South Korea (Bergermann and Göppert, 2000). For this project, the outer compression ring was built to be circular, and the shape of the inner ring was varied. It is shown in Figure 5 that 6 times more steel and 1.6 times more cable material were required when the inner ring is elliptical with the aspect ratio of 10:7. It was because "unnecessarily" high pre-tensioning forces, which led to larger cable members, were needed for the cables in the area where the bending angle of the rim is large. The increase of the pre-tensioning force and corresponding cable section was so high that more amount of the cable materials was needed even though the length of each cable member decreased, for the case with more elliptical inner ring. This thesis aims to generalize this finding by using a typical spoke wheel roof structure model and varying the aspect ratio of the inner and outer rings.

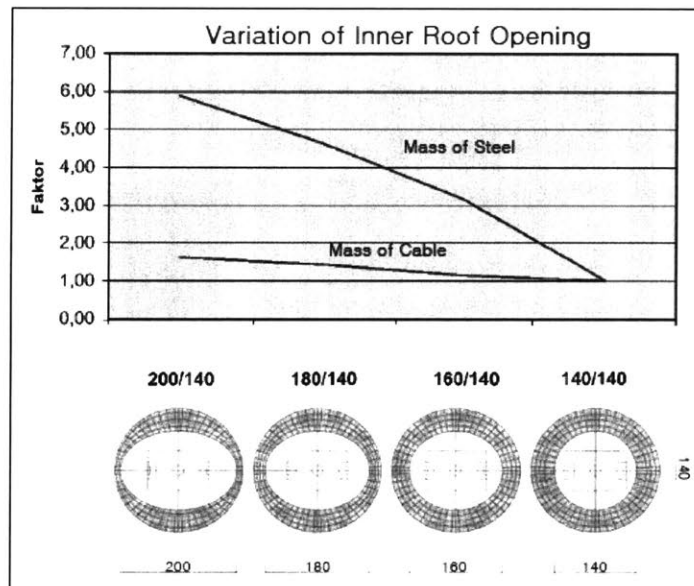


Figure 5. Variation of the inner ring and the corresponding amount of materials required for Pusan Dome in South Korea (Bergermann and Göppert, 2000)

Figure 6 summarizes the evolution of a spoke wheel roof system which included transformations of the inner and outer ring geometries and the variations of the oval shapes.

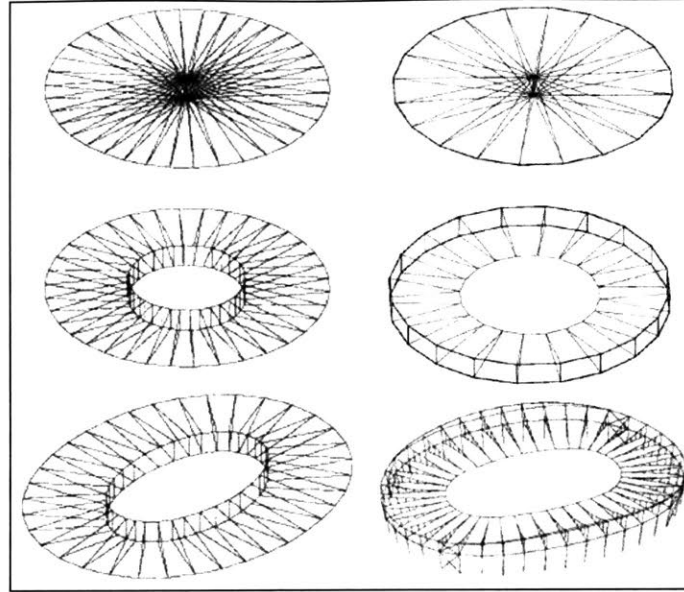


Figure 6. Evolution of a spoke wheel roof system (Bergermann and Göppert, 2000)

#### iv) Efficient Structure

Numerous approaches to "optimize" a structure have been introduced in order to determine and execute better designs of structures. Over the recent decades, cost has been the engineer's biggest concern (Mazurek, Baker, & Tort, 2010), and the general structural optimization problem has been to choose the design of minimal cost among the designs that meet certain constraints (Prager, 1970). Cost can be directly related to the volume of material when construction costs are ignored, and the minimization of structural volume can lead to an efficient structure.

In that context, Schlaich's work (Schlaich, 2010) proves how a spoke wheel roof system achieves light weight and the corresponding good efficiency. Galileo Galilei, in his book "The Discourses and mathematical demonstrations relating to two new sciences" published in 1638, introduced the square-cube law, which indicates that the bending capacity of a structure increases at a smaller rate than its span. Therefore, increase of the span of a structural member results in a significantly larger amount of materials required. However, this considerable increase in material use can be mitigated by using elements stressed by tension or compression, rather than by bending (Schlaich, 2010). While only the edge fibers of an element are fully stressed by bending, the entire cross-section is completely stressed and utilized under tensile or compressive stress, enabling axial members to have smaller cross-sectional areas. Schlaich also

mentioned that tension members are preferred to compression members because they are not subject to buckling, and pre-tensioning that can transform unfavorable compressive stress to tensile stress is ideal.

As discussed, a spoke wheel roof system resists loads primarily through axial forces, and pre-tensioning the radial spoke and tension rings ideally convert compression members into tension members. Therefore, a spoke wheel roof uses little amount of material weight, which leads to reduction of project cost and increase of structural efficiency. Moreover, it is usually built using repetitive modules due to its symmetrical shape, which makes its construction easier.

### **c) Literature Review**

Research over the past few decades has investigated the behaviors of a spoke wheel structure depending on its geometry, but the findings remain rather case-specific and qualitative.

In her Master's thesis, Boom (2012) explored the structural behavior of a spoke wheel roof system and the capability of its use as a stadium roof. She investigated the influence of several design variables on the strength and stiffness of the roof qualitatively. According to Boom (2012), less curvature, introduction of pre-tension in the spokes, smaller spoke spacing, larger cross-sectional area of the rim, and smaller radius of the rings lead to higher strength and stiffness of a roof. Moreover, rocker bearings are preferred over roller supports for financial and structural reasons. Cable structures perform the best for circular structures.

Boom (2012) conducted a detailed analysis of the Amsterdam Arena as a reference structure, by assigning loads and section and material properties based on the actual values. It was to determine the most efficient design among three different truss configurations with different diagonal positions which were designed by the author. Product of the absolute average deformation and average self-weight was used as the evaluation criterion for the structural efficiency of each variant. The efficient structure was decided to be the one with smaller evaluation criterion value. Building cost and constructability of a structure considering connection and support conditions were also discussed. It was found out that providing the connection or load path between the curved corner of the outer ring and the straight part of the inner ring, as shown in Figure 7-(a), resulted in the higher efficiency of the design, than when there was not such a connection as in Figure 7-(b). Also, the deformation increased at its straight edges, indicating that a non-circular shape of the rims negatively affects structural efficiency. However, it should be noted that the model used in Boom's thesis was significantly different from the one in the present thesis. Boom's modeled structure consisted of members which could also take bending moment, and the geometry of its inner and outer rings was closer to a rounded rectangle with straight edges at some parts, rather than an ellipse. Because of the geometry that included straight parts, using cables turned out to be

significantly less efficient than using trusses for this case, and it was recommended to use cables only when the rims do not possess any straight parts.

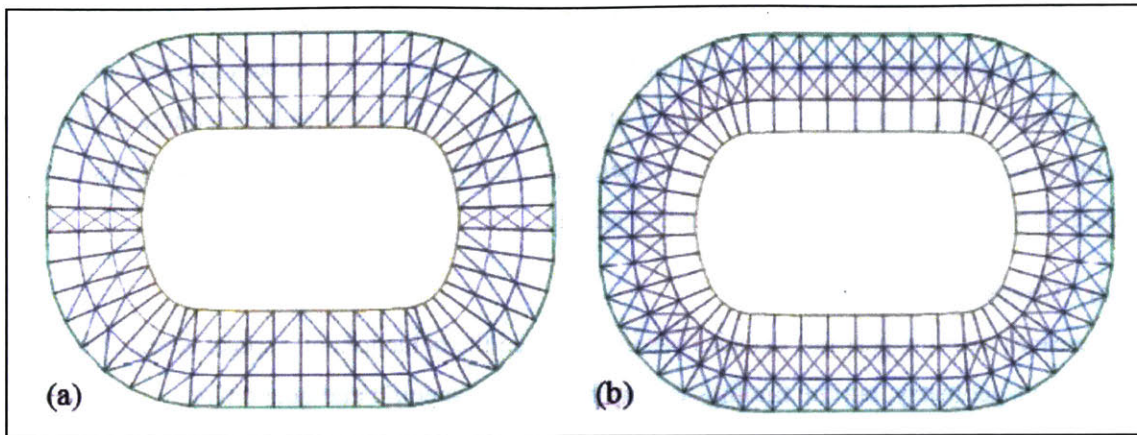


Figure 7. Ring and truss elements configurations in the thesis of Boom (2012): (a) “Variant 1” with members connecting the curved corner of the outer ring and the straight part of the inner ring, (b) “Variant 2” without such connecting members

Boom's thesis gave a great insight on how the variation of some design parameters would affect the structural behavior of a spoke wheel roof system, but it did not explain quantitatively how significant those effects were. On the other hand, the present study introduces numerical results in order to show how significant each variable is to the overall performance of a structure. Also, a structure using cable members and the influence of circular versus elliptical rims on the structural performance are explored.

Masubuchi (2013) introduced novel methods to fold retractable membranes to the rim of a stadium roof, not to its center. Because a spoke wheel roof system was often used for retractable roofs, the history and structural principles of the system were explained. However, detailed analysis focused on membranes rather than the frame, as its purpose was to propose new approaches to design membrane systems.

Bergermann and Göppert (2000), as discussed in the previous section, showed that the greater amount of materials would be required for the Pusan Dome when its inner ring became more elliptical. The material quantity was used to evaluate the efficiency of the structure.

#### **d) Precedents**

One of the first examples of spoke wheel roof structures is the American Pavilion designed by Edward Durell Stone and engineered by Blaton Aubert for 1958 Brussels Universal and International Exposition. With a spoke wheel roof principle, it achieved a large, column-free space which was ideal for exposition. Another early example is the roof of the Utica Memorial Auditorium, which is characterized by its dual pre-stressed cable system with the use of separation struts as shown in Figure 8. It was designed by Lev Zetlin in 1960, and is known to be the first example of using two layers of the suspended cables, which has been widely used afterwards. This design was designated as a National Historic Civil Engineering Landmark by the American Society of Civil Engineers (ASCE) in 2011 for its innovative roof structure. A more well-known example of the system is the roof of the Madison Square Garden in New York City, which was built in 1968. Figure 9 shows this roof designed by the structural engineer Fred Severud. Suspended cables spanning between an inner tension ring and an outer compression ring formed the roof, and they were post-tensioned by the self-weight of the decks above, as seen in Figure 9. This lightweight roof enabled a 425 ft-diameter, column-free span and imposed little weight for the supporting stadium structure, which had limited foundation support conditions as the Penn Station was positioned underground. The New York State Pavilion by Phillip Johnson in 1964 and the roof of the Oracle Arena by Skidmore, Owings and Merrill in 1966 are other early examples of using spoke wheel principles.

In the 1980s, central openings were introduced to spoke wheel roofs. One of the early examples is the Zaragoza Arena roof designed by Schlaich Bergermann Partner in 1988. The roof was added to cover the stands of the existing circular building which was first built for Spanish bull-fights in 1764. The roof had to be as light as possible to minimize the additional load from its weight onto the existing masonry structure, and retractable at its center. Such constraints led to the rediscovery and use of a spoke wheel roof system.

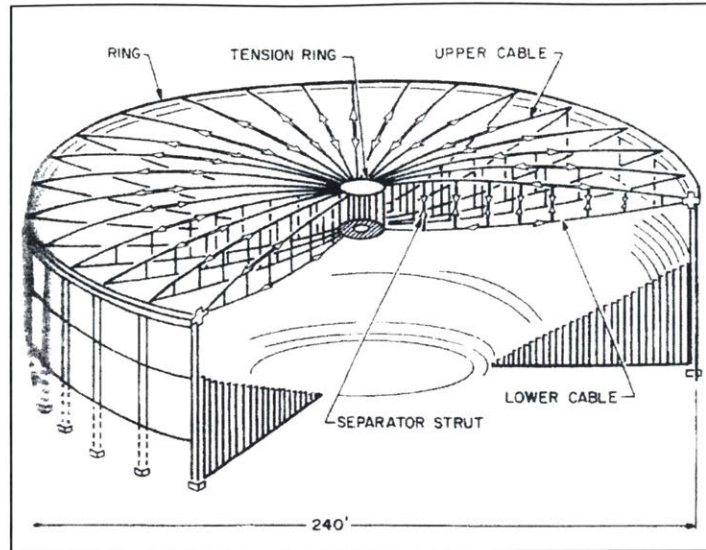


Figure 8. Utica Memorial Roof (Allen and Zalewski, 2010)

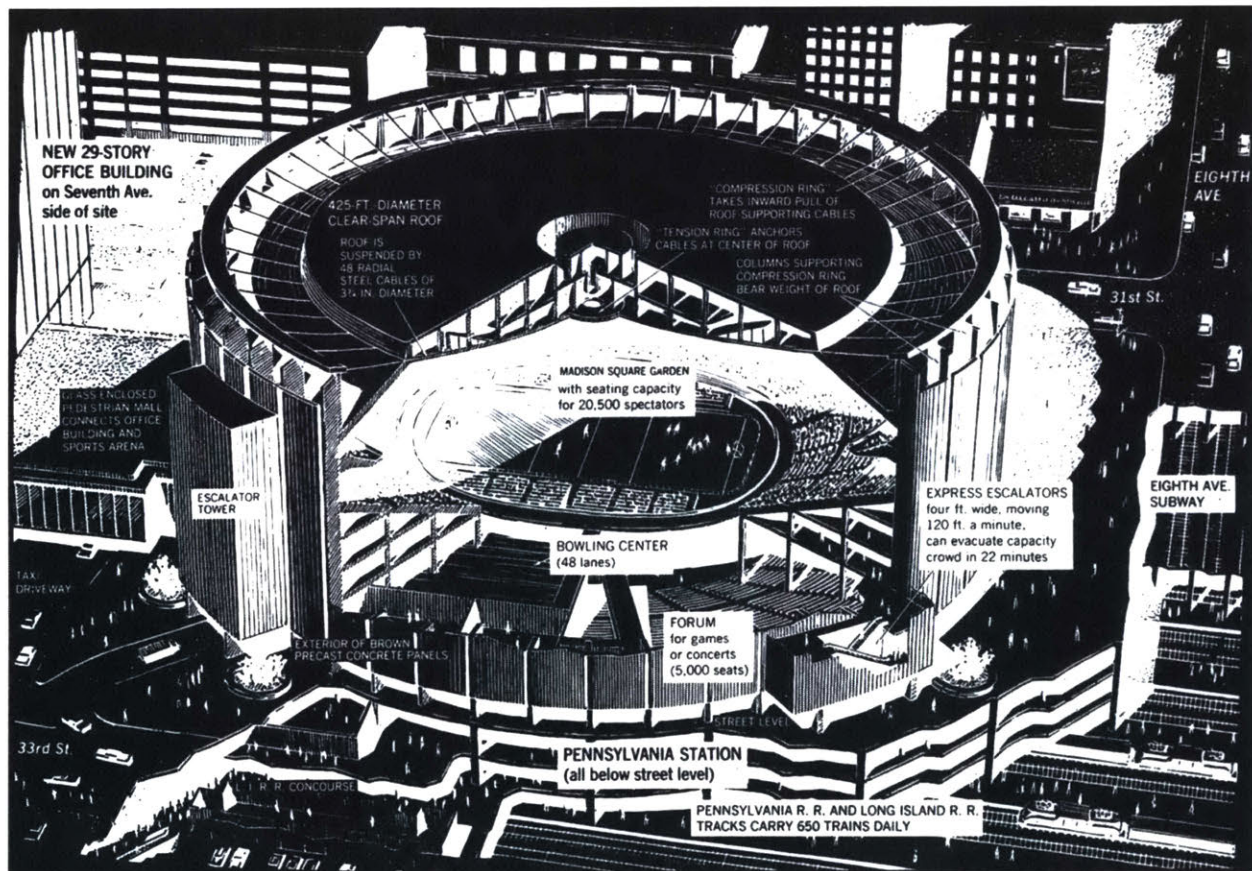
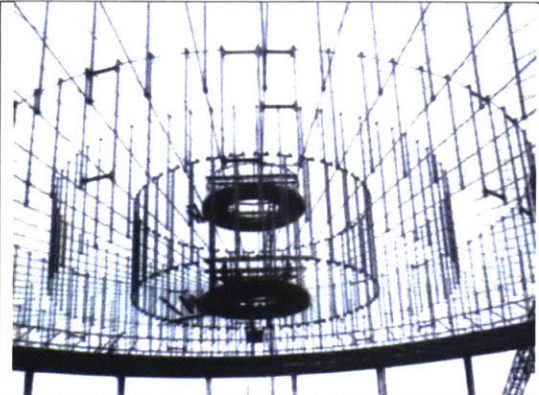



Figure 9. Roof Structure of the Madison Square Garden (Building with steel, 1968)

The following 20 arena or stadium roofs were investigated for their size and ring configuration as precedents using spoke wheel roof systems, accompanied by their photos in Figure 10-a to 10-t. The precedents are listed in the ascending order of their roof installation dates. Their shapes are categorized into circular and elliptical ones. Even if a shape is closer to a rounded rectangle than an ellipse, it is categorized as an elliptical shape for convenience. The diameters are also shown for some circular roofs of which published information on their dimension is available. All the listed precedents except for a, b, c, f, g, i, and r are projects engineered by Schlaich Bergermann Partner.

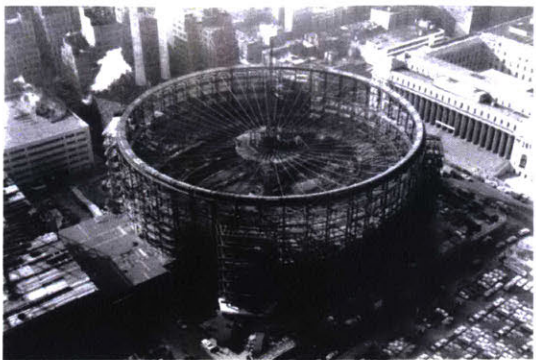
a. Utica Memorial Auditorium (1960)

	Stadium Name	Utica Memorial Auditorium ("The Aud")
	Location	New York, USA
	Roof Shape	Circular
	Roof Dimension	Diameter = 240 ft (Allen and Zalewski, 2010)
	Roof Area	45,220 ft <sup>2</sup>
	Completed Year	1960
	Ring Configuration	Two inner tension rings + One outer compression ring
Figure 10-a. Utica Memorial Auditorium (Source: <i>Utica Memorial Auditorium</i> [Photograph], Retrieved from <a href="http://www.columbia.edu/cu/gsap/BT/BSI/TENSEGRI/tensegri.html">http://www.columbia.edu/cu/gsap/BT/BSI/TENSEGRI/tensegri.html</a> )		


b. Palasport di Genova (1962)

	Stadium Name	Palasport di Genova
	Location	Genova, Italy
	Roof Shape	Circular
	Roof Area	41,530 ft <sup>2</sup>
	Completed Year	1962
	Ring Configuration	Two inner tension rings + One outer compression ring
Figure 10-b. Palasport di Genova (Source: Cepolina, F. (Photographer). (2014). <i>Genoa Palasport ceiling net</i> [Photograph], Retrieved from <a href="http://www.cepolina.com/Genoa-Palasport-ceiling-net.html">http://www.cepolina.com/Genoa-Palasport-ceiling-net.html</a> )		


c. Madison Square Garden (1968)

	Stadium Name	Madison Square Garden
	Location	New York, USA
	Roof Shape	Circular
	Roof Dimension	Diameter = 425 ft (Building with steel, 1968)
	Roof Area	128,120 ft <sup>2</sup>
	Completed Year	1968
	Ring Configuration	One inner tension ring + One outer compression ring (Stiffened by additional floor on top)
<p>Figure 10-c. Madison Square Garden (Source: <i>Madison Square Garden under Construction</i> [Photograph]. (1967). Retrieved from <a href="https://historiasdenuevayork.es/tag/madison-square-garden-under-construction/">https://historiasdenuevayork.es/tag/madison-square-garden-under-construction/</a>)</p>		

d. Plaza de Toros of Zaragoza (1988)

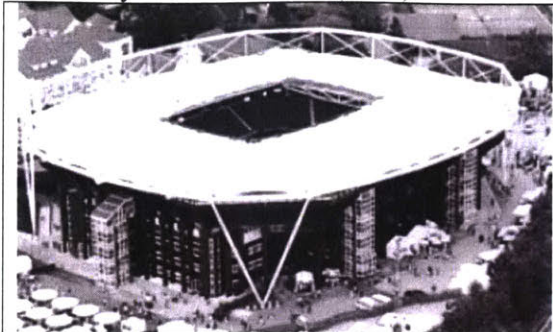
	Stadium Name	Plaza de Toros de Zaragoza
	Location	Zaragoza, Spain
	Roof Shape	Circular
	Roof Dimension	Diameter = 246 ft (Schlaich Bergemann Partner)
	Roof Area	47,360 ft <sup>2</sup> + 10,760 ft <sup>2</sup> (fixed + retractable)
	Completed Year	1764, 1988 (roof added)
	Ring Configuration	Two inner tension rings + One outer compression ring
<p>Figure 10-d. Plaza de Toros of Zaragoza (Source: schlaich bergemann partner. (Photographer). <i>Bull ring roof Zaragoza (Plaza de Toros)</i> [Photograph], Retrieved from <a href="http://www.sbp.de/en/project/bull-ring-roof-zaragoza-plaza-de-toros/">http://www.sbp.de/en/project/bull-ring-roof-zaragoza-plaza-de-toros/</a>)</p>		

e. Mercedes-Benz Arena (1993)


	Stadium Name	Mercedes-Benz Arena (former Gottlieb-Daimler-Stadion)
	Location	Stuttgart, Germany
	Roof Shape	Elliptical
	Roof Area (ft <sup>2</sup> )	365,970+38,540 (fixed + retractable)
	Completed Year	1933, 1993 (roof added)
	Ring Configuration	One inner tension ring + Two outer compression rings
<p>Figure 10-e. Mercedes-Benz Arena (Source: Storck, M. (Photographer). <i>Gottlieb-Daimler-Stadium</i> [Photograph], Retrieved from <a href="http://www.sbp.de/en/project/gottlieb-daimler-stadium/">http://www.sbp.de/en/project/gottlieb-daimler-stadium/</a>)</p>		




f. Gerry Weber Stadium (1994)

	Stadium Name	Gerry Weber Stadium
	Location	Halle, Germany
	Roof Shape	Elliptical
	Roof Area	75,350 ft <sup>2</sup>
	Completed Year	1994
	Ring Configuration	One inner tension ring + Two outer compression rings
	Figure 10-f. Gerry Weber Stadium (Bergermann and Göppert, 2000)	


g. De Kuip (Feyenoord Stadium) (1994)

	Stadium Name	De Kuip
	Location	Rotterdam, Netherlands
	Roof Shape	Elliptical
	Roof Area	181,500 ft <sup>2</sup> (approx.)
	Completed Year	1938, 1994 (renovated)
	Ring Configuration	Two inner tension ring (offset) + One outer compression ring
	Figure 10-g. De Kuip (Boom, 2012)	


h. Bukit Jalil National Stadium (NSC Roof Outdoor Stadium Kuala Lumpur) (1997)

	Stadium Name	Bukit Jalil National Stadium (NSC Roof Outdoor Stadium Kuala Lumpur)
	Location	Kuala Lumpur, Malaysia
	Roof Shape	Elliptical
	Roof Area	414,410 ft <sup>2</sup>
	Completed Year	1996, 1997 (roof added)
	Ring Configuration	Two inner tension rings + One outer compression ring
	Figure 10-h. Bukit Jalil National Stadium (Source: <i>NSC Roof Outdoor Stadium Kuala Lumpur</i> [Photograph], Retrieved from <a href="http://www.sbp.de/en/project/nsc-roof-outdoor-stadium-kuala-lumpur/">http://www.sbp.de/en/project/nsc-roof-outdoor-stadium-kuala-lumpur/</a> )	


i. Estadio Olimpico (Olympic Stadium Seville) (1999)

	Stadium Name	Estadio Olimpico (Olympic Stadium Seville)
	Location	Sevilla, Spain
	Roof Shape	Elliptical
	Roof Area	269,100 ft <sup>2</sup>
	Completed Year	1952, 1999 (roof added)
	Ring Configuration	One inner tension ring + Two connection levels at an outer compression ring + Membrane as structural member
<p>Figure 10-i. Estadio Olimpico (Source: <i>Olympic Stadium Seville</i> [Photograph], Retrieved from <a href="http://www.sbp.de/en/project/olympic-stadium-seville/">http://www.sbp.de/en/project/olympic-stadium-seville/</a>)</p>		


j. Volkspark Stadium Hamburg (HSH Nordbank Arena) (2000)

	Stadium Name	Volkspark Stadium Hamburg (HSH Nordbank Arena)
	Location	Hamburg, Germany
	Roof Shape	Elliptical
	Roof Area	376,740 ft <sup>2</sup>
	Completed Year	1953, 2000 (roof added)
	Ring Configuration	One inner tension ring + One outer compression ring + Secondary structure to support membranes
<p>Figure 10-j. Volkspark Stadium Hamburg (Source: Coddou, R. (Photographer). <i>Volkspark Stadium Hamburg</i> [Photograph], Retrieved from <a href="http://www.sbp.de/en/project/volkspark-stadium-hamburg/">http://www.sbp.de/en/project/volkspark-stadium-hamburg/</a>)</p>		


k. Pusan Sports Dome (2001)

	Stadium Name	Pusan Sports Dome
	Location	Pusan, S. Korea
	Roof Shape	Circular
	Roof Area	365,970 ft <sup>2</sup>
	Completed Year	2001
	Ring Configuration	Two inner tension rings + One outer compression ring
	Figure 10-k. Pusan Sports Dome (Source: schlaich bergemann partner. (Photographer). <i>Pusan Dome</i> [Photograph], Retrieved from <a href="http://www.sbp.de/en/project/pusan-dome/">http://www.sbp.de/en/project/pusan-dome/</a> )	

l. Volkswagen Arena (2002)

	Stadium Name	Volkswagen Arena
	Location	Wolfsburg, Germany
	Roof Shape	Elliptical
	Roof Area	161,460 ft <sup>2</sup> + 86,110 ft <sup>2</sup> (fixed + retractable)
	Completed Year	2002
	Ring Configuration	Two inner tension rings + One outer compression ring
	Figure 10-l. Volkswagen Arena (Source: <i>Volkswagen-Arena-Wolfsburg</i> [Photograph], Retrieved from <a href="http://www.euoplan-online.de/volkswagen-arena/stadion-109.html">http://www.euoplan-online.de/volkswagen-arena/stadion-109.html</a> )	

m. National Athletics Stadium Abuja (2003)

	Stadium Name	National Athletics Stadium Abuja
	Location	Abuja, Nigeria
	Roof Shape	Elliptical
	Roof Area	355,210 ft <sup>2</sup>
	Completed Year	2003
	Ring Configuration	Two inner tension rings + One outer compression ring
	Figure 10-m. National Athletics Stadium Abuja (Source: <i>National Athletics Stadium Abuja</i> [Photograph], Retrieved from <a href="http://www.sbp.de/en/project/national-athletics-stadium-abuja/">http://www.sbp.de/en/project/national-athletics-stadium-abuja/</a> )	

n. Commerzbank Arena (2006)

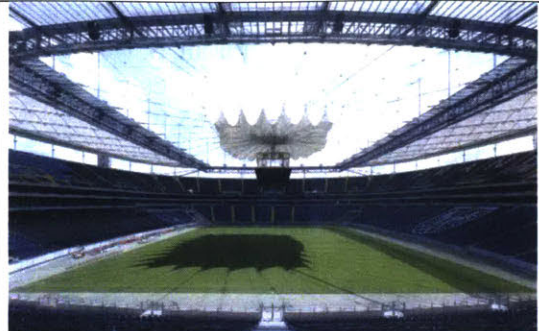
	Stadium Name	Commerzbank Arena
	Location	Frankfurt, Germany
	Roof Shape	Elliptical
	Roof Area	312,150 ft <sup>2</sup> + 86,110 ft <sup>2</sup>
	Completed Year	1925, 2006 (roof added)
	Ring Configuration	Two inner tension rings + One outer compression ring

Figure 10-n. Commerzbank Arena (Source: fantastic new media gmbh. (Photographer). *Commerzbank-Arena Frankfurt (former Waldstadion)* [Photograph], Retrieved from <http://www.sbp.de/en/project/commerzbank-arena-frankfurt-former-waldstadion/>)

o. Bay Arena Leverkusen (2009)


	Stadium Name	Bay Arena Leverkusen
	Location	Leverkusen, Germany
	Roof Shape	Circular
	Roof Dimension	Diameter = 705 ft (Schlaich Bergermann Partner)
	Roof Area	301,390 ft <sup>2</sup>
	Completed Year	1958, 2009 (roof added)
	Ring Configuration	One inner tension ring + Two outer compression rings

Figure 10-o. Bay Arena Leverkusen (Source: Bayer 04 Leverkusen Fußball GmbH. (Photographer). *BayArena Leverkusen* [Photograph], Retrieved from <http://www.sbp.de/en/project/bayarena-leverkusen/>)

p. Jawaharlal Nehru Stadium (2009)




	Stadium Name	Jawaharlal Nehru Stadium
	Location	Delhi, India
	Roof Shape	Elliptical
	Roof Area	484,380 ft <sup>2</sup>
	Completed Year	1983, 2009 (roof added)
	Ring Configuration	One inner tension ring + Two outer compression rings

Figure 10-p. Jawaharlal Nehru Stadium (Source: *JNS Jawaharlal Nehru Stadium* [Photograph], Retrieved from <http://www.sbp.de/en/project/jns-jawaharlal-nehru-stadium/>)

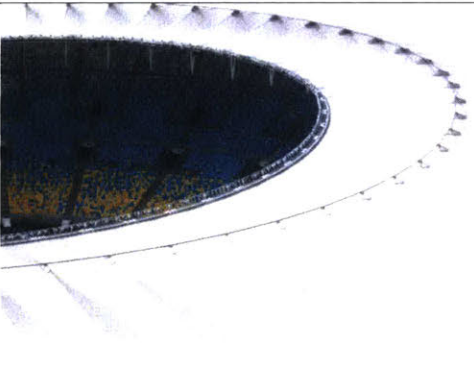
q. Moses Mabhida Stadium (2009)

	Stadium Name	Moses Mabhida Stadium
	Location	Durban, S. Africa
	Roof Shape	Elliptical
	Roof Area	495,140 ft <sup>2</sup>
	Completed Year	2009
	Ring Configuration	One inner tension ring + One outer compression ring + Arch
	Figure 10-q. Moses Mabhida Stadium (Source: schlaich bergemann partner. (Photographer). <i>Moses Mabhida Stadium</i> [Photograph], Retrieved from <a href="http://www.sbp.de/en/project/moses-mabhida-stadium/">http://www.sbp.de/en/project/moses-mabhida-stadium/</a> )	


r. The Forum (2010)

	Stadium Name	The Forum
	Location	California, USA
	Roof Shape	Circular
	Roof Dimension	Diameter = 407 ft
	Roof Area	130,200 ft <sup>2</sup> (approx.)
	Completed Year	1966, 2014 (roof renovated)
	Ring Configuration	Two inner tension rings + One outer compression ring
Figure 10-r. The Forum (Source: INGLEWOOD - <i>The Forum</i> [Photograph], Retrieved from <a href="http://www.skyscrapercity.com/showthread.php?p=110702389">http://www.skyscrapercity.com/showthread.php?p=110702389</a> )		

s. Maracanã Stadium (2013)

	Stadium Name	Maracanã Stadium
	Location	Rio de Janeiro, Brazil
	Roof Shape	Elliptical
	Roof Area	45,700 ft <sup>2</sup>
	Completed Year	2013
	Ring Configuration	One inner tension ring + Three outer compression rings (Two of which are intermediate)
Figure 10-s. Maracanã Stadium (Source: Bredt, M. (Photographer). <i>Stadium Maracanã (Estádio Jornalista Mário Filho)</i> [Photograph], Retrieved from <a href="http://www.sbp.de/en/project/stadium-maracana-estadio-jornalista-mario-filho/">http://www.sbp.de/en/project/stadium-maracana-estadio-jornalista-mario-filho/</a> )		

t. Stadium FK Krasnodar (2015)

	Stadium Name	Stadium FK Krasnodar
	Location	Krasnodar, Russia
	Roof Shape	Elliptical
	Roof Area	259,410 ft <sup>2</sup>
	Completed Year	2015
	Ring Configuration	One inner tension ring + Two outer compression rings
	<p>Figure 10-t. Stadium FK Krasnodar (Source: Bredt, M. (Photographer). <i>Stadium FK Krasnodar</i> [Photograph], Retrieved from <a href="http://www.sbp.de/en/project/stadium-fk-krasnodar/">http://www.sbp.de/en/project/stadium-fk-krasnodar/</a>)</p>	

## 2. Methodology and Model

### A. Methodology

#### a) Platform

This thesis aims to determine the influence of geometric changes on the overall structural performance of the structure. To immediately find out the effect of the variables on the behaviors, parametric modeling is implemented.

For parametric modeling, Rhinoceros-Grasshopper is used as a platform for the model. Rhinoceros (Robert McNeel & Associates, Version 5) is a 3-dimensional computer graphics software, and Grasshopper (Robert McNeel & Associates, Version 0.9.0076) is a visual generative algorithm-building application within Rhino. In order to conduct structural analysis in the platform, Karamba (Clemens Preisinger, Version 1.2.2), a Finite Element Analysis (FEA) tool which is embedded in the parametric modeling settings of Grasshopper, is also used (Preisinger, 2016).

#### b) Analysis Procedure

Additional attention is paid to the analysis procedure and the Grasshopper-Karamba model, because a spoke wheel roof system model involves members with pre-tensioning force. For the analysis, the materials are assumed to be linear-elastic.

##### i) Effect of Pre-tension

When analyzing a structure, a modeled state refers to the idealized particular state of the structure. On the other hand, analyzed states are acquired after loads are applied and the structure deforms to reach equilibrium. While the unstressed state, where all the inner actions are zero, is commonly used for a modeled state, such a state does not exist for pre-stressed structures and cannot be used. Therefore, stressed states, where the inner actions are not zero, can be used to analyze pre-stressed structures. (Ghisbain, 2013)

For the analysis of a pre-tensioned structure, the pre-tension forces within the members are first turned into equivalent loads onto their nodes. Then the model is analyzed regularly under the actual and equivalent loads. In the last step, the equivalent loads are removed and the pre-tension forces are added to the axial forces attained through the regular analysis (Ghisbain, 2013).

The validity of this analysis method can be proved through the following equations, using the displacement method.

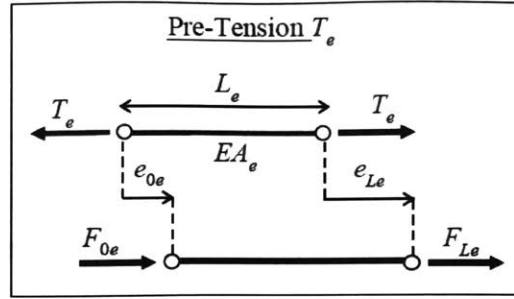


Figure 11. Pre-tensioned truss element (Ghisbain, 2013)

For a truss element with its local end actions  $F_{0e}$  and  $F_{Le}$  and displacements  $e_{0e}$  and  $e_{Le}$  with pre-tension  $T_e$  as shown in Figure 11, the equilibrium requires

$$\bar{F}_e = \underline{K}_e \bar{E}_e + \bar{T}_e$$

where  $\bar{F}_e$  = local end actions vector,  $\bar{E}_e$  = local displacement vector,  $\bar{T}_e$  = element pre-tension vector, and  $\underline{K}_e$  = element stiffness matrix.

With  $\bar{U}_e$  = global displacement vector,  $\bar{R}_e$  = rotation vector, and  $\bar{P}_e$  = global end actions vector =  $\underline{R}_e^T \bar{F}_e$ ,

$$\bar{F}_e = \underline{K}_e \underline{R}_e \bar{U}_e + \bar{T}_e$$

$$\bar{P}_e = \underline{R}_e^T \underline{K}_e \underline{R}_e \bar{U}_e + \underline{R}_e^T \bar{T}_e$$

The total end actions are therefore

$$\bar{P} = \left( \sum_e \underline{R}_e^T \underline{K}_e \underline{R}_e \right) \bar{U} + \left( \sum_e \underline{R}_e^T \bar{T}_e \right) = \underline{K} \bar{U} + \bar{T}$$

Where  $\underline{K}$  = global stiffness matrix,  $\bar{U}$  = node displacement vector, and  $\bar{T}$  = pre-tension force vector.

With  $\bar{Q}$  = applied load vector,

$$\bar{Q} = \underline{K} \bar{U} + \bar{T}$$

$$\bar{U} = \underline{K}^{-1} (\bar{Q} - \bar{T})$$

From the equations above, it is indicated that the pre-tension acts on the structure as equivalent loads when the node displacements are determined.



The axial force in an element is the same as the local end action.

$$F_{Le} = (0 \ 1)\overline{F}_e = (0 \ 1)(\underline{K}_e \overline{E}_e + \overline{T}_e) = (0 \ 1)\underline{K}_e \underline{R}_e \overline{U}_e + \overline{T}_e$$

The equations above show that the pre-tension force should be added to the axial force acquired from the previous analysis to get the final axial force of the element that is pre-tensioned.

In the spoke wheel roof model with pre-tensioned spokes, tension ring(s) and radial spokes are designed to be pre-tensioned. The magnitude of the pre-tension assigned to each cable member should be equal to or greater than the maximum compressive force induced to it. In order to determine the amount of pre-tension required and the final axial forces in the elements based on the theory above, the following analysis procedure in Figure 12 is executed. For the Step A, applied loads and load cases are determined as will be discussed in Section 2.B.g.

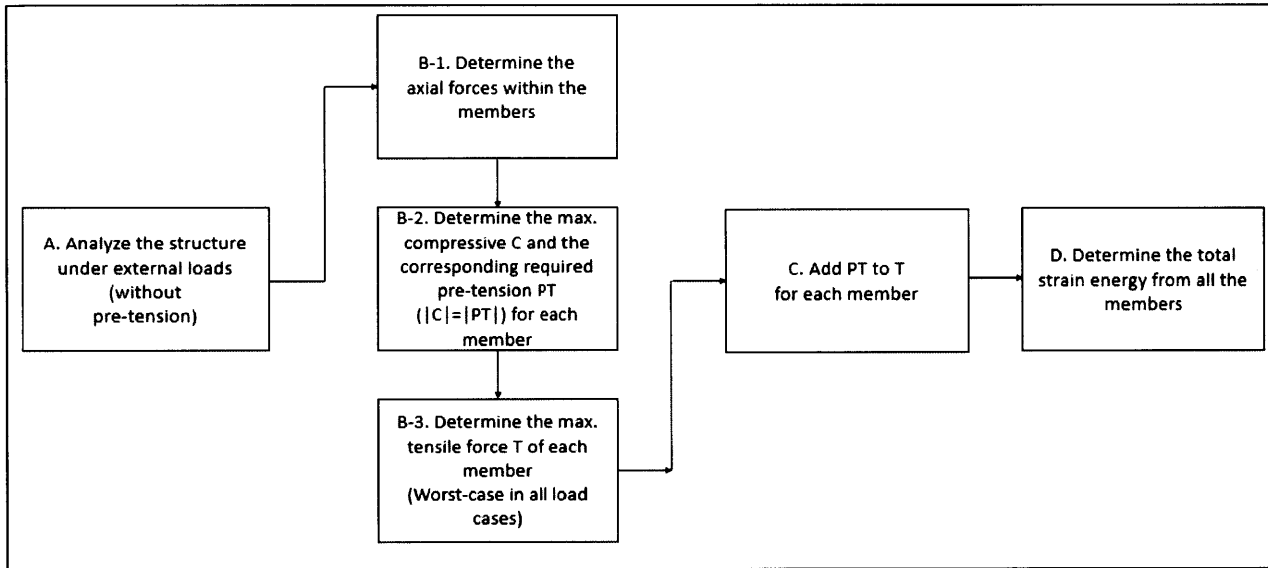


Figure 12. Analysis procedure considering pre-tension

Pre-tensioning an element gives it geometric stiffness to resist loads in the transverse direction. Therefore, the geometric stiffness which accounts for the existing forces and the deformation contributes to the total stiffness of a pre-tensioned structure.

$$\underline{K}_{total} = \underline{K}_P + \underline{K}_G$$

where  $\underline{K}_{total}$ = total stiffness matrix,  $\underline{K}_P$ = physical stiffness matrix, and  $\underline{K}_G$ = geometric stiffness matrix.

The geometric stiffness only relates to the transverse actions whereas the physical stiffness considers axial actions. For a truss element, the axial and transverse actions can be uncoupled. (Ghisbain, 2013) Therefore, the geometric stiffness does not influence the final axial force and can be ignored in the model to calculate the load path factor, the evaluation criterion for the structural efficiency in this thesis.

## **ii) Grasshopper-Karamaba**

In order to successfully model a structure with pre-tensioned cable members and implement the procedure laid out in Figure 12, the following components and their settings are used in Grasshopper-Karamaba.

“Modify Element” component is used to turn the members of the model into truss elements by setting “Bending” to false and setting their bending stiffness to zero. This is necessary because all the members of the model are assumed to be axial members under either tension or compression.

“Buckling” is set to false and turned off for the cable members. In a spoke wheel roof system, the cable members should be provided pre-tension, of which the magnitude should be equal to or greater than the maximum compressive force that may be generated in any load case. Because the given pre-tension counter-balances such compressive force, the cable members are not subject to compression and buckling. By disabling buckling of the cable members, the maximum compressive force induced to those members can be successfully obtained, and it is enabled to “simulate pre-tensioned, slender elements without having to really pre-tension them” (Preisinger, 2016).

A randomly large number is assigned to “NII”, the Second Order Theory Normal Force, which is required to stabilize the system for the first step of the Second Order Theory analysis in Karamaba. The value is updated through the iteration during the analysis, unless the maximum number of equilibrium iterations, or MaxIter value of the analysis component is set to zero. For this thesis, MaxIter is assigned zero, so that it is constant over the variation of geometry and provide relatively constant and valid results. In Karamaba, the NII value, which gives geometric stiffness to the system, is independent from the axial force  $N$  generated from the external loads (Preisinger, 2016). Therefore, the randomly assigned NII value does not affect the analysis procedure in Figure 12 to obtain the final load path of the members.

In combination with the “Modify Element” component, “Analyze Th. II” component is used to evaluate the structure considering the second order theory (Th. II) as shown in Figure 13. This analysis component accounts for the geometric stiffness, or the stabilizing effect of the tensile forces within the members. It is based on the assumption of small displacements and relatively constant axial forces, correspondingly (Preisinger, 2016).

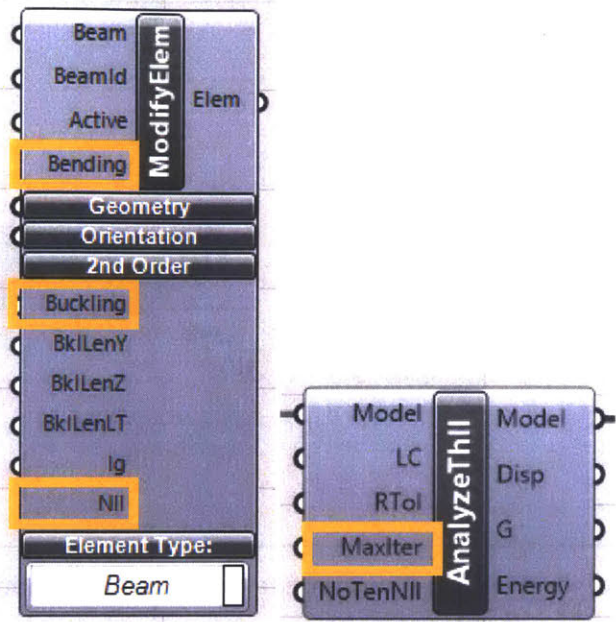


Figure 13. Modify Element and AnlyzeThII components in Grasshopper-Karamba

## B. Model

### a) Reference Project

The roof of the Zaragoza Arena built in 1988 in Zaragoza, Spain, shown in Figure 10-d, is chosen as the reference project. This structure is selected because the information on the dimension of the roof and its structural members is available. It is also perfectly circular, which is appropriate for a base model from which geometric variations are applied.

As seen in the schematic drawing in Figure 14, The Zaragoza arena roof is characterized by one outer compression ring, two inner tension rings, and pre-tensioned spokes (Schlaich Bergermann Partner, n.d.). As discussed in the previous section, both this configuration and the alternative one with two outer compression rings and one inner tension ring are explored.

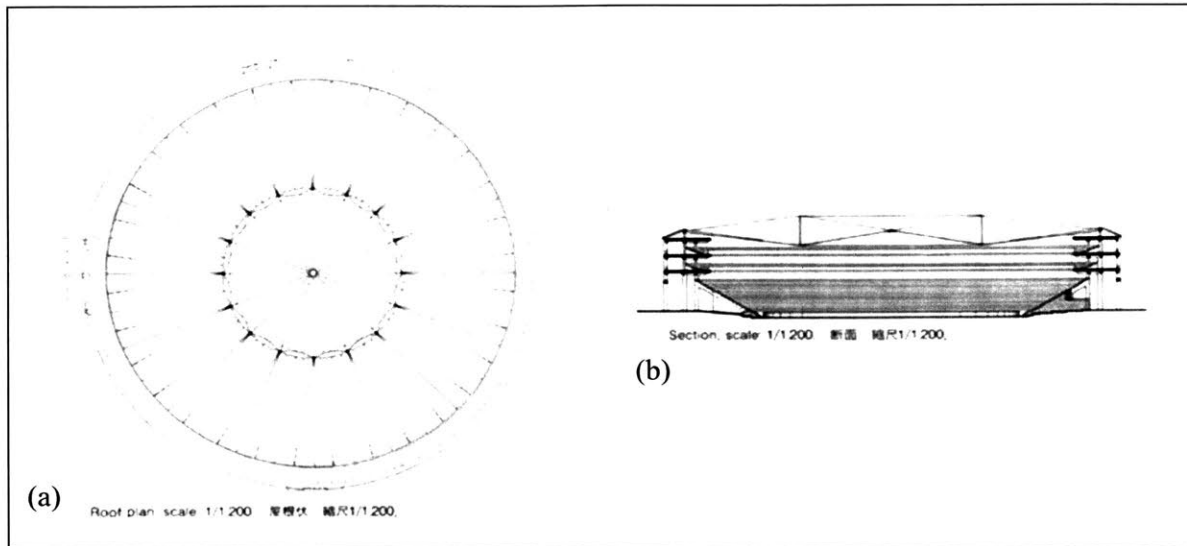


Figure 14. Drawings of the Zaragoza Arena roof: (a) plan and (b) elevation views (Holgate, 1997)

The inner and outer diameters of the Zaragoza Arena roof are approximately 36m (118 ft) and 82.7m (271 ft), respectively. The compression ring is made of rectangular steel tube (800 x 500 mm or 31.5 x 19.7 in) sections filled with concrete, which adds sufficient dead load to counteract uplift wind forces. Two inner tension rings that are made with 60 mm (2.4 in) locked coil rope are spaced 6 m (20 ft) apart and connected by 210 mm (8.3 in) - diameter steel tube vertical struts. Inner and outer rings are connected by 32 upper radial cables of 36 mm (1.4 in) diameter and 64 lower radial cables of 26 mm (1 in) diameter, stretching 23.35 m (76.6 ft). The radial cables are anchored to the rings by simple pin connections. Slopes for the upper and lower radial cables are the same, because uplift wind and downward snow loads are approximately equal. Pre-stressing level of the radial cables was decided so that under the maximum upward or downward load, the force in upper or lower cables is reduced to zero, in order to minimize the cable forces and cross sections (Schlaich Bergermann Partner, n.d.).

The membrane or roof covering, made of polyester and coated with PVC, is placed on the lower spokes. The area of the entire roof structure covers the area of 5,400 m<sup>2</sup> (58,125 ft<sup>2</sup>) of which 1,000 m<sup>2</sup> (10,764 ft<sup>2</sup>) is retractable.

Although the Zaragoza Arena roof was the reference project, a few modifications are made to further simplify and optimize the model for the thesis. Such modifications are outlined in the following sections 2.B.b - g.

### b) Ring Configuration

The reference project has two inner tension rings and one outer compression ring. In this thesis, both that configuration and the other one with one inner tension ring and two outer compression rings are explored.

Configuration 1: Two inner tension rings + One outer compression ring + Pre-tensioned radial spokes

Configuration 2: One inner tension ring + Two outer compression rings + Pre-tensioned radial spokes

For either case, the roof covering membrane is assumed to be attached to the spokes which are sloped downwards towards the rim. Accordingly, the membrane is designed to be on the upper spokes for Configuration 1, and on the lower spokes for Configuration 2, as seen in Figure 15. The position of the membrane determines which spokes the wind and snow loads are applied to.

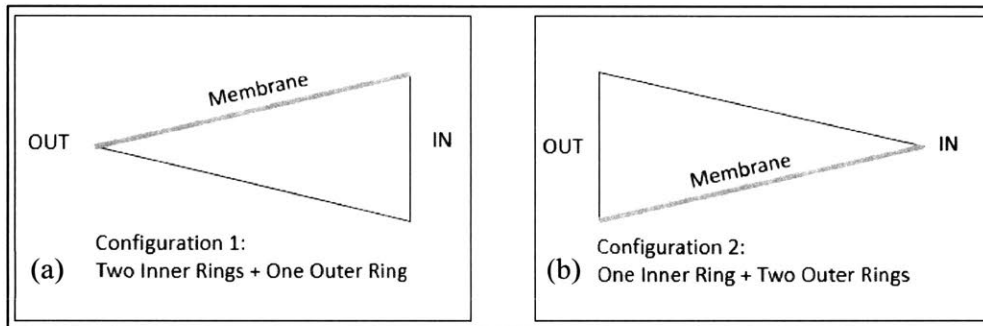


Figure 15. Membrane position for the two configurations: (a) Configuration 1 and (b) Configuration 2

To provide transverse stiffness to the cables over the long span, additional vertical ties or struts between the upper and lower cables are necessary. Spacing of those members is decided based on the thesis of Ivar Boom (Boom, 2012), which set it to be between 7.02 m (23.03 ft) and 7.31 m (24.00 ft), referring to the design of the Amsterdam Arena as shown in Figure 7. In the present thesis, the vertical struts or ties are provided between the inner and outer rings, with spacing that varies between 17 ft and 25 ft. At the locations of the vertical members, additional tension rings are provided to increase the stability of the structure, along the spokes with the downwards slopes towards the outer rim as seen in Figure 16.

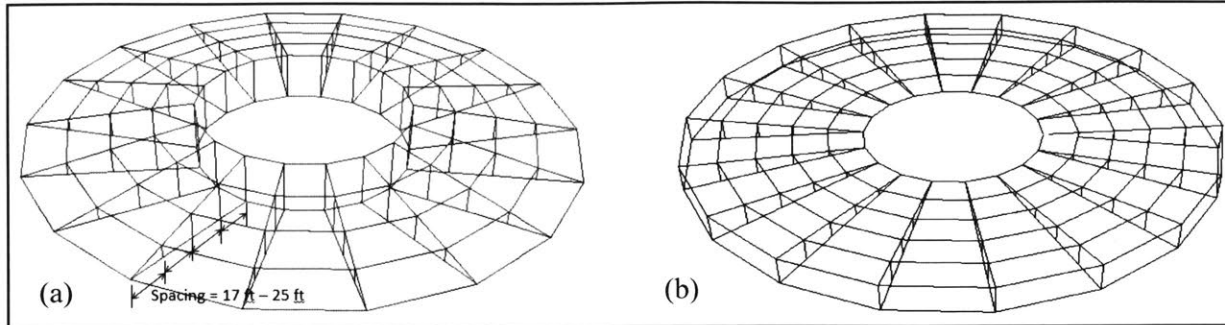


Figure 16. Spacing between the vertical struts or ties: (a) Configuration 1 and (b) Configuration 2

### c) Material and Section Properties

The reference project, the Zaragoza Arena roof, built in 1988, has a steel box filled with concrete as a section for the compression ring. On the other hand, it became more common to use only steel for the compression ring for the later projects, including the Mercedes-Benz Arena built in 1993. For this thesis, every member in the model is assumed to be made of steel to simplify the model. The primary purpose of the thesis lies in comparing different geometries in terms of their structural performance. Therefore, it is a valid approach to set the material of the members to be the same for each geometric configuration and have the material as an independent variable.

The evaluation criterion of the structural performance in this thesis is decided to be load path factor. This concept will be discussed in more details in Section 2.C.b. By keeping the material and cross-sectional properties the same for each member throughout the designs with geometric variation, only the axial force and length of each member affect the load path for each design. Therefore, the material and section properties do not influence the results of this thesis, provided that they are sufficient to withstand the external loads applied to the structure.

The material and section properties of the members are decided based on the Mercedes-Benz Arena, designed by Arat Siegel und Partner and engineered by Schlaich Bergermann Partner, due to the availability of this information (Boom, 2012). These properties are used consistently over various geometric settings. Although the base geometry for the model is the Zaragoza Arena, the size of the model can become significantly larger than the original size through the process of parametric modeling. Because the Mercedes-Benz Arena is approximately 7.7 times larger by the roof area than the Zaragoza Arena, using the material and section properties based on the former can guarantee the stability of the structure with various geometric settings. This conservative choice of the section properties is valid, since the evaluation criterion for the structural performance is not affected by the cross-sections as will be discussed in Section 2.C.b.

All the members are decided to have circular cross sections, based on the typical sections of the reference projects of the Zaragoza Arena and Mercedes-Benz Arena roofs. For the cable members of the roof model, strength is a leading criterion over flexibility. Therefore, a locked coil which consists of several interlocked coils is used due to its high strength.

The material properties used are summarized in Table 1.

Table 1. Material properties for the model

<b>Material</b>			
	Young's Modulus (E)	Density	Yield Strength (fy)
<b>Cable Elements</b>	29,000 ksi	0.484 k/ft <sup>3</sup>	257 ksi
<b>All Other Elements</b>	29,000 ksi	0.484 k/ft <sup>3</sup>	50 ksi

**d) Connection**

All the members of the model are designed as members carrying axial forces only. They are assigned pin connections at their nodes to ensure the successful axial force transfer, and based on the reference project of the Zaragoza Arena roof.

**e) Supports**

The columns that connect the outer rim to the ground, or the top of the supporting structure, are not included in the model. This part of the structure is neglected because primary purpose of the thesis is to see the influence of the ring geometry on the overall performance of the structure. The columns are not included also to reduce the number of parameters, as the height of the columns and their support conditions could be additional variables.

Since the columns are excluded from the model, the points where the columns would have been connected to the outer rim are given supports. In order to provide the outer ring freedom for radial translation, the supports are modeled as rollers, except for four of them which are to be pin supports as shown in Figure 17. The pin supports are provided to prevent the translation in the global x- and y-direction and to stabilize the structure.

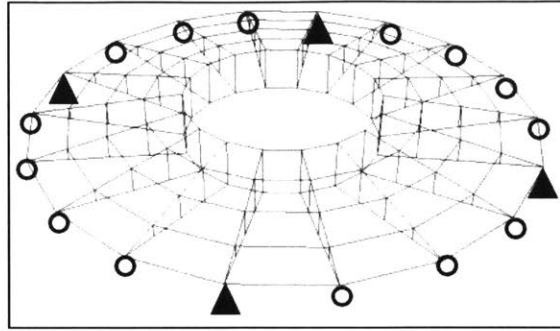


Figure 17. Support conditions for the outer ring, where circles and triangles show roller and pin supports, respectively

#### f) Location

The reference project Zaragoza Arena is in Zaragoza, Spain. However, the model for the thesis is assumed to be in the United States, in order to apply the American Building Codes with which the author was more familiar. Another reason is to associate the research more with the structural engineering industry in the United States, where the spoke wheel roof systems are more scarce than in Europe.

The location of the roof model is decided to be New York City, USA. New York City is at a similar latitude as Zaragoza, Spain, and both cities are located in coastal regions.

Climate analysis is done to compare the climate for the two cities using Ladybug (Mostapha Sadeghipour Roudasri, Version 0.0.64), the environmental analysis plug-in for Grasshopper. Ladybug uses standard EnergyPlus Weather file (EPW files). The weather information is gathered from regional meteorological organizations over the world. Figure 18 shows the dry bulb temperature in Zaragoza and New York City. Both cities have similar climate, with hot summer and cold winter, although the climate in New York City has colder winters and is more dramatic with larger changes in temperature. The average temperature over a year for Zaragoza and New York City are 57.7 and 53.8 degrees Fahrenheit (14.3 and 12.1 degrees Celsius), respectively.



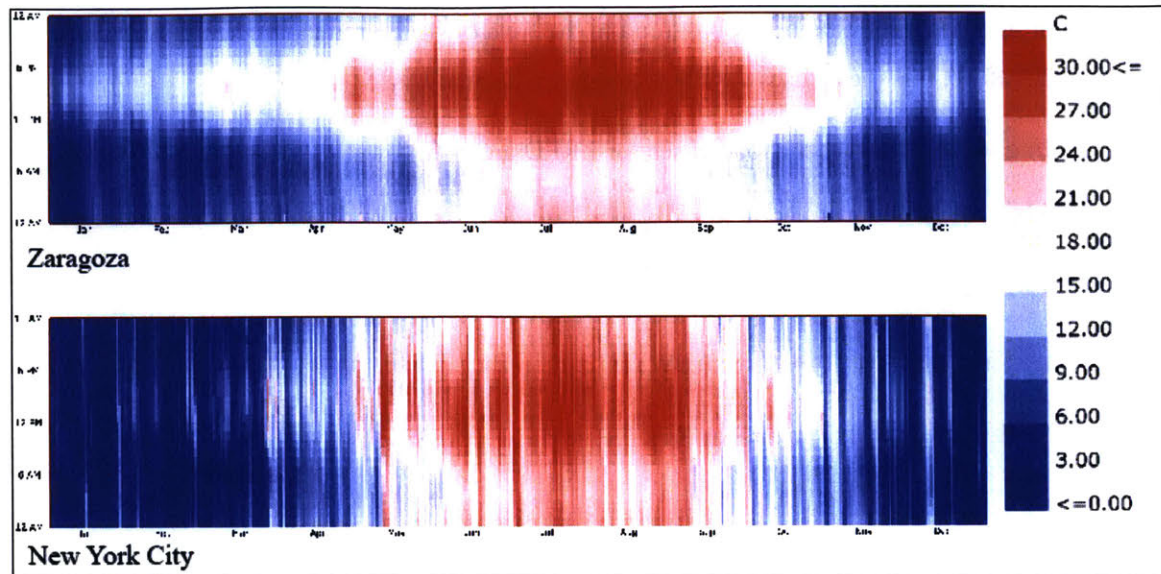


Figure 18. Annual dry bulb temperature in Zaragoza, Spain (top) and New York City, USA (bottom)

One of the most important climatic factors for structural engineering is the wind profile. Due to the lack of wind profile for Zaragoza, the weather data for Madrid, its closest city which has wind data available and similar geography around, is used instead. The average wind speed for Madrid and New York City are 2.44 and 5.18 meter per second (5.46 and 11.59 miles per hour) respectively. As New York City has a higher average wind speed, setting the location of the model to be New York City, USA results in greater wind loads applied to the model, larger internal forces within the members, therefore more conservative results in terms of wind loading, than setting the location to be Zaragoza, Spain.

#### g) Building Code and Loads

In order to analyze the stability and behavior of the model, it is necessary to apply appropriate loads to it. For the detailed analysis, the 2014 New York City Building Code (NYC BC) and the American Society of Civil Engineers Minimum Design Loads for Buildings and Other Structures, 2010 (ASCE 7-10) are used to determine respective loads. As the model location is New York City, NYC BC becomes the primary reference.

#### i) Load Cases

Between Allowable-stress design (ASD) and Load and Resistance Factor Design (LRFD), LRFD is used for the analysis for this thesis. ASD considers both the material and load uncertainties in a single factor of safety, whereas LRFD separates those uncertainties based on probability theory. Research has shown that using LRFD over ASD can lead to cost savings of projects and more efficient design, and

LRFD or similar approaches are being global trend in the field of structural engineering (Aghayere & Vigil, 2009). Therefore, this thesis uses LRFD throughout the analysis.

According to ASCE 7-10, the load cases for LRFD are as follows:

- a.  $1.4D$
- b.  $1.2D + 1.6L + 0.5(Lr \text{ or } S \text{ or } R)$
- c.  $1.2D + 1.6(Lr \text{ or } S \text{ or } R) + (L \text{ or } 0.5W)$
- d.  $1.2D + 1.0W + L + 0.5(Lr \text{ or } S \text{ or } R)$
- e.  $1.2D + 1.0E + L + 0.2S$
- f.  $0.9D + 1.0W$
- g.  $0.9D + 1.0E$

For the analysis of the model, only dead (D), snow (S), and wind load with two cases (W1, W2) are considered, which will be explained in more details in the upcoming sections 2.B.g.ii - vii. Therefore, the following load combinations are extracted from above and explored in this thesis.

0.  $1.4D$
1.  $1.2D + 1.6S + 0.5W1$
2.  $1.2D + 1.6S + 0.5W2$
3.  $1.2D + 1.0W1 + 0.5S$
4.  $1.2D + 1.0W2 + 0.5S$
5.  $0.9D + 1.0W1$
6.  $0.9D + 1.0W2$

#### **ii) Dead Load**

Dead loads consist of the weights of the structural members and objects that are permanently attached to the structures. The structural weight of each member was considered by the "Gravity Load" component in Rhino-Grasshopper-Karamba, based on their material and section properties which are pre-assigned.

Additionally, the weight of the membrane roof covering is considered. PVC-coated polyester is a typical membrane material and was taken for the model based on the reference project. Its weight (Masubuchi, 2013) is applied as dead load to the roof model in the direction of gravity.

$$\text{Membrane Roof Covering (PVC – coated Polyester, Type III): } 1 \left( \frac{\text{kg}}{\text{m}^2} \right) = 0.205 \text{ (psf)}$$

### iii) Wind Load

Wind load is caused when the wind is blocked by a structure, and its kinetic energy is transformed into pressure. The wind load depends on the velocity of the air, direction of the wind, geometry and stiffness of the structure, and the roughness of the surface.

NYC BC 2014 designates that the Chapter 6 of ASCE 7 shall be used to determine the wind loads. The numbers shown in parentheses next to the equations or values are the corresponding section numbers of ASCE 7-10.

### Wind Pressure

The ASCE 7-10 Standard expresses the wind velocity pressure equation as follows, with consideration of the importance and height of the structure and its surrounding terrain condition (ASCE 7-10, 2010, Section 30.3.2).

$$q_z = 0.00256 K_z K_{zt} K_d V^2 \text{ (psf)} \quad (1)$$

where

V = basic wind speed (miles per hour) (Section 26.5)

K<sub>z</sub> = velocity pressure exposure coefficient. (Section 30.3.1)

K<sub>zt</sub> = topographic factor (Section 26.8)

K<sub>d</sub> = wind directionality factor (Section 26.6)

q<sub>h</sub> = wind pressure at height h (psf)

### Risk Category (Section 1.5)

The model, designed as a stadium roof, is assigned a risk category of **II** because it imposed medium-high risk to human life in the event of failure, but it is not expected to disrupt a day-to-day civilian life or substantial hazard to the community in case of failure.

### **Basic Wind Speed (Section 26.5)**

According to the Section 1609.3 of the NYC BC, the basic wind speed for New York City is 98 miles per hour.

### **Directionality Factor $K_d$ (Section 26.6)**

$K_d = 0.85$ , as the roof model can be considered as a main wind force resisting system.

It is a calibrated factor for the case when wind load was acting in combination with other loads.

### **Topographic Factor $K_{zt}$ (Section 26.8)**

$K_{zt} = 1.0$ , as the model is assumed to be on flat ground.

### **Velocity pressure exposure coefficient $K_z$ (Section 30.3.1)**

The model is categorized as an exposure group C. Accordingly,

$$K_z = 2.01 \left( \frac{z}{z_g} \right)^{\frac{2}{\alpha}} \geq 2.01 \left( \frac{15}{z_g} \right)^{\frac{2}{\alpha}} = 0.84 \quad (2)$$

where  $\alpha = 9.5$  and  $z_g = 900$  ft (Section 26.9)

Based on the above values,

$$\therefore q = 24.17 \text{ psf}$$

### **Design wind pressures**

For the design of the roof, wind pressures considering outward and inward suction are considered as follows:

$$p = qGC_p - q_iGC_{pi} \text{ (psf)} \quad (3)$$

where  $q = q_h$ ,

$G$  = gust-effect factor = 0.85 (Section 26.9),

$C_p$  = external pressure coefficient (Section 27.4),

$(GC_{pi})$  = internal pressure coefficient (Section 26.11)

**Internal Pressure Coefficient ( $GC_{pi}$ ) (Section 26.11)**

$(GC_{pi}) = \pm 0.55$  for a partially enclosed building.

ASCE 7-10 specifies that the extreme cases, when either positive or negative values of  $(GC_{pi})$  are applied to all internal surfaces, should be considered to calculate the critical load condition. Plus and minus signs represent pressure towards and away from the roof surface.

**External pressure coefficient  $C_p$  (Section 27.4)**

Based on the typical geometry of model,  $C_p = -0.3$  (windward) and  $-0.18$  (leeward)

**Critical Load Conditions**

Figure 19 shows the two different load cases, the one with external suction on both roof sides, and the other with internal and external suction on the windward and leeward sides.

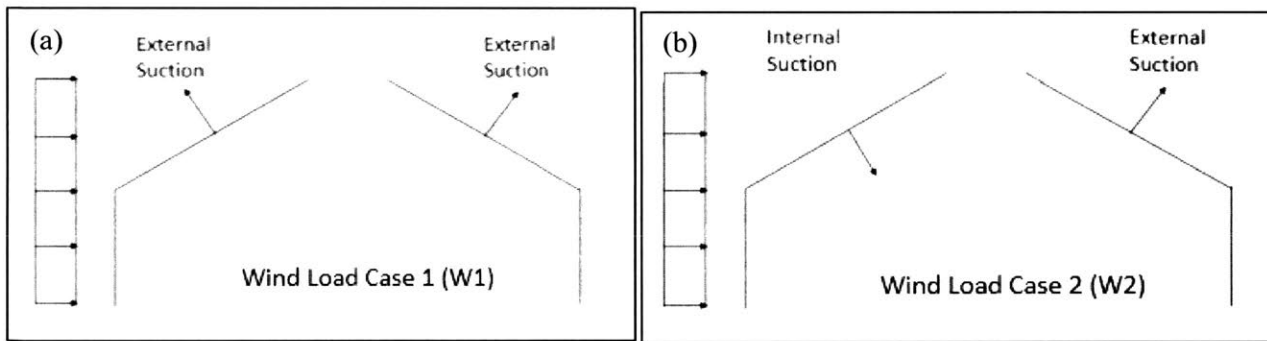


Figure 19. Wind load critical conditions: (a) Wind Load Case 1 (W1) and (b) Wind Load Case 2 (W2)

For each case, the wind load is calculated as in the following table.

Table 2. Wind load for windward and leeward sides

Wind Load Case	Windward Side	Leeward Side
W1	-19.46 psf (external suction)	-16.99 psf (external suction)
W2	+7.13 psf (internal suction)	-16.99 psf (external suction)

Wind suction loads are applied onto the membrane. Therefore, they are applied in the local z-, or local vertical direction as shown in Figure 20.

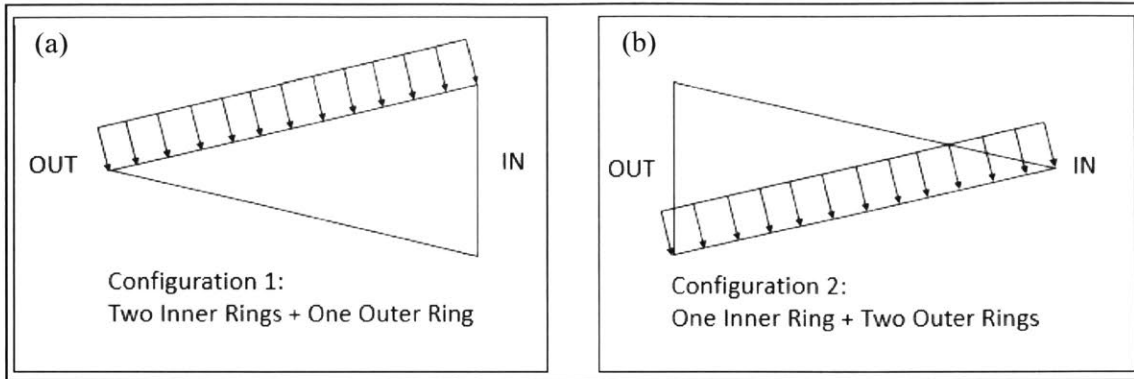


Figure 20. Wind load application for (a) Configuration 1 and (b) Configuration 2

#### iv) Snow Load

The flat roof snow load is defined as in Equation 4 (ASCE 7-10, 2010, Section 7.3).

$$p_f = 0.7 C_e C_t I_s p_g \text{ (psf)} \quad (4)$$

where

$C_e$  = Exposure factor (Section 7.3) = 0.9 for a fully exposed roof

$C_t$  = Thermal factor (Section 7.3) = 1.0 for a regular roof

$I_s$  = Importance factor (Section 1.5) = 1.0 for a risk category II

$p_g$  = Ground snow loads (Section 7) = 25 psf for New York City.

$$\therefore p_f = 0.7(0.9)(1.0)(1.0)(25) = 15.75 \text{ (psf)}$$

For a sloped roof, the snow load is defined as

$$p_s = C_s p_f \quad (5)$$

where  $C_s$  = warm roof slope factor = 1.0 (Section 7.4.1)

$$\therefore p_s = (1.0)(15.75) = 15.75 \text{ (psf)}$$

Snow loads are applied in the direction of gravity, on the spokes where the membrane is assumed to be attached, as seen in Figure 21.

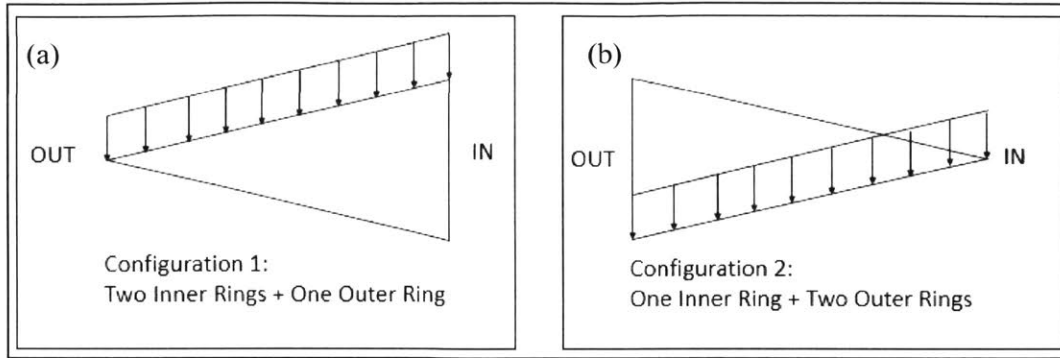


Figure 21. Snow load application for (a) Configuration 1 and (b) Configuration 2

**v) Live Load**

Live loads are induced by the weights of the objects that are temporarily applied to a structure or natural forces. Their magnitude is determined by the code based on the history of their impacts on existing structures. Because the live load that a spoke wheel roof structure experiences is insignificant, it is not considered for the analysis.

**vi) Rain Load**

As discussed in Section 2.B.b, the roof covering is placed on the spokes that are sloped downwards towards the rim. Due to substantial drainage path and membrane slope, rainwater accumulation on the membrane and corresponding rain load are assumed to be negligible. Based on the reference project of the Zaragoza Arena roof, the model has a membrane slope of approximately

$$\text{Slope} = \tan^{-1} \left( \frac{3m}{41.5m} \right) \cong 4 \text{ degrees} \quad (6)$$

Ponding instability is not considered in this case as well, because the membrane slope is significantly larger than 1.19 degrees prescribed for ponding-susceptible-bays defined in ASCE 7-10, Section 8.4.

**vii) Seismic Load**

Seismic load comes from the structure's distortion and its lateral distortion, when the ground motion is caused by earthquakes. This thesis only explores the spoke wheel roof systems, which are not major lateral force resisting systems and are often “added” to the stadium structures below. The base stadium structures other than the roof are assumed to take the seismic load, so it is not considered for the analysis of the model in this thesis.

### C. Variables and Objective

#### a) Variables

The following parameters are used as variables to modify the overall geometry of a spoke wheel roof system and explore the corresponding change in structural performance. Other tentative variables such as material or cross section of the members are not considered, in order to limit the scope of the research to the geometry of the spoke wheel roof system.

#### i) Ring Configuration

As discussed in the Chapter 2, two ring configurations are explored.

Configuration 1: Two inner tension rings + One outer compression ring + Pre-tensioned radial spokes

Configuration 2: One inner tension ring + Two outer compression rings + Pre-tensioned radial spokes

#### ii) Radii of the Inner and Outer Rings

In order to determine the influence of the roof span on the performance, the radii of the inner ( $r_1$ ) and outer rings ( $r_2$ ) are varied. One of them is varied while the other was constant over various roof spans. The roof span is defined as the difference between the outer and inner ring radii.

Masubuchi (2013), with the courtesy of Schlaich Bergermann Partner, stated that a spoke wheel roof system uses fewer materials than a conventional cantilevered roof, when the roof span is bigger than 35 m (115 ft), as seen in Figure 22. Therefore, the minimum roof span for the model is decided to be 115 ft. Figure 22 also shows that the efficiency of a spoke wheel roof is less dependent on its scale, while the efficiency of a cantilevered roof significantly reduces when its size becomes larger.

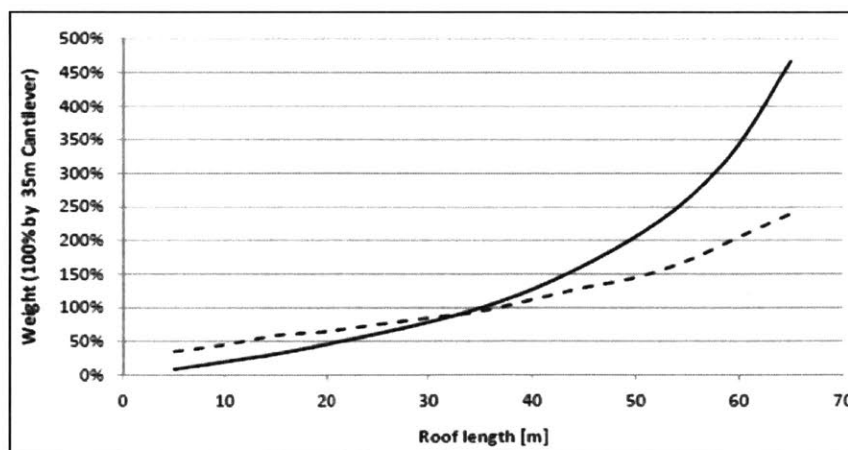


Figure 22. Structural weight comparison: cantilevered (solid line) vs. spoke wheel structure (dotted line) (Masubuchi, 2013)



### **iii) Aspect Ratio**

As a spoke wheel roof system is mostly used for stadia, it is sometimes inevitable to make it non-circular for architectural reasons. Considering that a system may be oval, aspect ratio is decided as one of the variables.

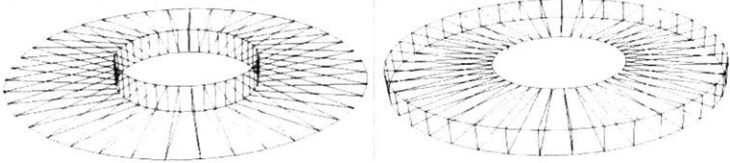
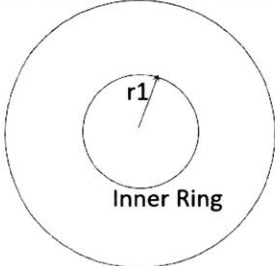
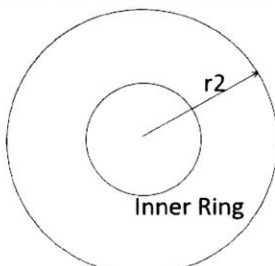
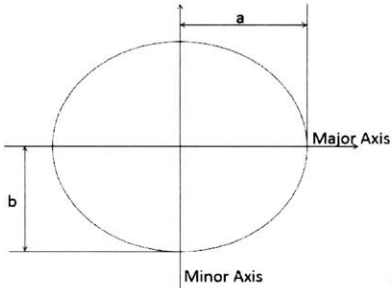
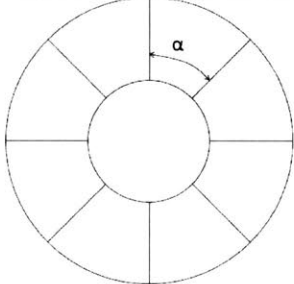
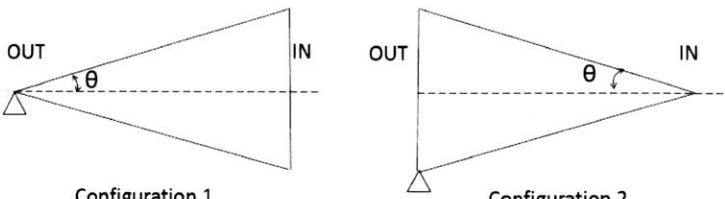
The aspect ratio for an ellipse is the ratio of the major axis to the minor axis. In this thesis, it is represented in the form of a fraction. For example, the aspect ratio of a circle is 1:1, but it is shown as 1 in this thesis for convenience.

### **iv) Spoke Spacing and Slope**

As discussed in Section 1.B.b, radial stiffness of a spoke wheel roof system largely depends on the spoke properties. Therefore, the spacing ( $\alpha$ ) and slope ( $\theta$ ) of the spokes are treated as variables. They are both measured as angles. The spacing of the spokes is directly related to the number of the spokes, and the slope of the spokes is related to the distance between the double inner or outer rings. The slope of the spoke is measured from the center plane of the entire structure to the spokes. The upper and lower spokes are assumed to be at the same angle, making the variable of slope of the spokes applicable to both the upper and lower spokes.

The variables used are summarized in Table 3.

Table 3. Geometric variables for the design

	Variable	Details
1	Ring Configuration (Configuration 1, Configuration 2)	 <p style="text-align: center;">Configuration 1                      Configuration 2</p>
2	Diameter of the Inner Ring ( $r_1$ )	
3	Diameter of the Outer Ring ( $r_2$ )	
4	Aspect Ratios of the Inner ( $R(r_1)$ ) and Outer ( $R(r_2)$ ) Rings	 <p style="text-align: right;"><math>R = a / b</math></p>
5	Spacing of the Spokes ( $\alpha$ ) (related to Number of the Spokes)	
6	Slope of the Spokes ( $\theta$ ) (related to Distance between the Double Rings)	 <p style="text-align: center;">Configuration 1                      Configuration 2</p>

## b) Evaluation Criterion

As discussed in Section 1.B.b.iv regarding efficient structures, minimal structural volume indicates minimal material cost and therefore an efficient, well-performing structure.

Michell (1904) first studied on the minimization of structural volume and stated that the minimal volume of a frame structure is achieved when all the members are at their allowable stresses and their virtual strains are maintained under a certain prescribed value (Michell, 1904). Other approaches included joint coordinates determination through geometry and differential equations and topology optimization (Mazurek et al., 2010). In the present thesis, the approach introduced in the paper by Mazurek, Baker, and Tort (2010) is used. The authors start with Maxwell's Theorem on Load Paths, shown in Equation 7, which were also the foundation of Michell's study in 1904. For a truss structure where only tension and compression forces exist,

$$\sum F_T L_T - \sum F_C L_C = \sum \vec{F} \cdot \vec{r} \quad (7)$$

where  $F_T$  and  $L_T$  are force and length of each tension member and  $F_C$  and  $L_C$  are those of each compression member, respectively.  $\vec{F}$  is the external forces applied to the structure and  $\vec{r}$  is the position vector of those forces.

When both sides of the equation are divided by the allowable stress of material,  $\sigma$ , the volume can be obtained.

$$V_{\text{Total}} = V_{\text{Tension}} + V_{\text{Compression}} = \frac{\sum F_T L_T}{\sigma} + \frac{\sum |F_C| L_C}{\sigma} \quad (8)$$

Based on Equation 8, Stromberg, Beghini, Baker, and Paulino (2012) expressed the problem of minimizing structural volume as

$$\min_x V = \min_x \frac{1}{\sigma} \sum |P| \cdot L \quad (9)$$

where  $x$  = vector of design variables,

$\sigma$  = allowable stress of the material used,

$P$  = internal force of each member,

and  $L$  = length of each member.

Baker, Beghini, L.L., Mazurek, Carrion, and Beghini, A. (2013) referred to a part of Equation 9, the sum of the internal force and length of each member, as “Load Path” (Baker et al., 2013).

$$\text{Load Path} = \sum |P| \cdot L \quad (10)$$

According to Equations 9 and 10, minimizing the load path of a structure results in the minimization of its structural volume or weight (Baker et al., 2013).

A load path is a path through which a load is transferred from its point of application on the structure to the foundation (Aghayere & Vigil, 2009). The minimization of the load path can lead to the minimization of the structural volume and the corresponding cost, resulting in an “efficient” structure. The model in the present thesis is assumed to use the same material for each member throughout different cases with various geometric settings and consists of the members that are in either tension or compression. Therefore, decreasing load path can indicate that a more efficient structure with less structural volume and cost can be achieved.

In the present thesis, two different allowable stress values are used:  $\sigma_c = 257$  ksi for cable members and  $\sigma_o = 50$  ksi for all other members, where the former is about five time larger than the latter. Therefore, based on Equation 9, the problem of minimizing volume can be expressed as

$$\min_x V = \min_x \frac{1}{\sigma} \sum |P| \cdot L = \min_x \left( \frac{1}{\sigma_c} \sum |P_{cable}| \cdot L_{cable} + \frac{1}{\sigma_o} \sum |P_{others}| \cdot L_{others} \right) \quad (11)$$

where  $P_{cable}$  and  $L_{cable}$  are internal force and length of a cable member and  $P_{others}$  and  $L_{others}$  are those of a member which is not cable.

Considering that the internal force of an element is in kips and its length is in feet, the corresponding load path can be calculated as

$$\begin{aligned} \text{Load Path} &= lp_i = lp_i \text{ of cable members} + lp_i \text{ of all other elements} \\ &= \left( \frac{1}{5} \right) \sum |P_{cable}| \cdot L_{cable} + \left( \frac{1}{1} \right) \sum |P_{others}| \cdot L_{others} \end{aligned} \quad (12)$$

In this thesis, the overall size of the roof structure varies depending on the variable settings. For that reason, the load path value of each case is divided by its total projected roof area for normalization as shown in Equation 13, so that the comparison among various cases becomes easier.

$$\text{Normalized Load Path} = lp'_i = \frac{lp_i}{A_T} \quad (13)$$

where  $A_T =$  projected area of the roof ( $\text{ft}^2$ ).

In order to represent the results unit-less, the normalized load path is normalized again, being divided by the “base value” in the data set, and named to be “Load Path Factor”. The base value is the smallest value of the objective, in this case the smallest load path factor value, in the data set.

$$\text{Load Path Factor} = LP_i = \frac{lp_i'}{lp_0'} \quad (14)$$

where  $LP_i$  = load path factor for the i-th case,

$lp_i'$  = normalized load path for the i-th case,

and  $lp_0'$  = smallest normalized load path in the dataset.

For example, as will be discussed more in Section 3.A, when the inner ring radius  $r_1$  is set at 59 ft and the outer ring radius  $r_2$  varies from 174 ft to 294 ft, the load path is the smallest when the outer ring radius is 174 ft. This smallest objective value is designated to be the “base value” of the dataset acquired from varying  $r_2$ . The load path of each case with  $r_1 = 59$  ft and varying  $r_2$  is divided by that base value to get the “Load Path Factor”, as shown in Table 4 and Equations 14 to 16.

Table 4. Sample calculation of load path factors

Variable: Outer Ring Radius ( $r_2$ )	Inner Ring Radius ( $r_1$ ) (ft)	Outer Ring Radius ( $r_2$ ) (ft)	Load Path	Load Path Factor
Case 1	59	174	48.92 [ $lp_0'$ , “Base Value”]	1.00 [Eq 15]
Case 2	59	178	49.32	1.01 [Eq 16]
Case n	59	$r_{2n}$	$lp_n'$	$lp_n'/48.92$ [Eq 17]

$$LP_1 = \frac{lp_1'}{lp_0'} = \frac{48.92}{48.92} = 1.00 \quad (15)$$

$$LP_2 = \frac{lp_2'}{lp_0'} = \frac{49.32}{48.92} = 1.01 \quad (16)$$

$$LP_n = \frac{lp_n'}{lp_0'} = \frac{lp_n'}{48.92} \quad (17)$$

To summarize, the Load Path Factor is calculated by normalizing the load path twice, first by the total roof area and later by the “base value” in the dataset, and is used as an evaluation criterion.

As discussed in Section 1.B.b.iv, a structure can be considered to be efficient when it uses minimal materials. Therefore, a smaller load path factor that leads to a reduced volume of material indicates a more efficient structure.

It is noted that the cross-sectional areas of the elements do not affect the calculation of the load path factor. Also, adoption of the load path as an evaluation criterion is possible because all the members of the model are assumed to be subject only to axial forces.

### 3. Results

The model is run in Rhino-Grasshopper-Karamba with different geometric settings.

It turns out that Load Case 6, when wind load case W2 or the internal suction from the wind is fully considered, is the governing case for both of the configurations. It indicates that the consideration of a climate and the corresponding wind loads is crucial for the design of a spoke wheel roof system.

While both inner and outer radii are two of the variables, their starting dimensions are decided to be 59 ft and 174 ft, respectively. They are based on the reference project of the Zaragoza Arena and the research by Schlaich Bergermann Partner (Masubuchi, 2013) that a spoke wheel roof system becomes more efficient than a traditional cantilever roof when the roof span is at least 35 m (115 ft). The following variable settings are used as the starting case for all the variable settings.

Table 5. Starting variable settings

Inner Ring Radius, $r_1$ (ft)	59
Outer Ring Radius, $r_2$ (ft)	174
Number of Spokes	18
Height between the Double Rings, $d$ (ft)	30

#### A. Change of Inner and Outer Ring Radii

To determine the influence of the ring radii on the performance, inner ( $r_1$ ) and outer ( $r_2$ ) radii are varied, while both inner and outer rings are maintained to be perfectly circular. First, the inner radius is fixed at 59 ft and the outer one is changed from 174 ft to 294 ft. Accordingly, the difference between the inner and outer radii, or the roof span, is from 115 ft to 235 ft. Second, the outer ring radius is set at 255 ft and the inner radius is varied from 20 ft to 140 ft. The outer radius here is set to be different from the starting value shown in Table 5, in order to achieve the same roof span range from 115 ft to 235 ft, from the case when  $r_2$  is a variable. Both configurations (C1 and C2) are tested.

Figure 23 shows the influence of the inner and outer radii ( $r_1$  or  $r_2$ ) and different configurations (C1 or C2) on the performance. For example, “C1; $r_1$ ” in the legend means that the data is acquired for the Configuration 1, by varying the inner ring radius.

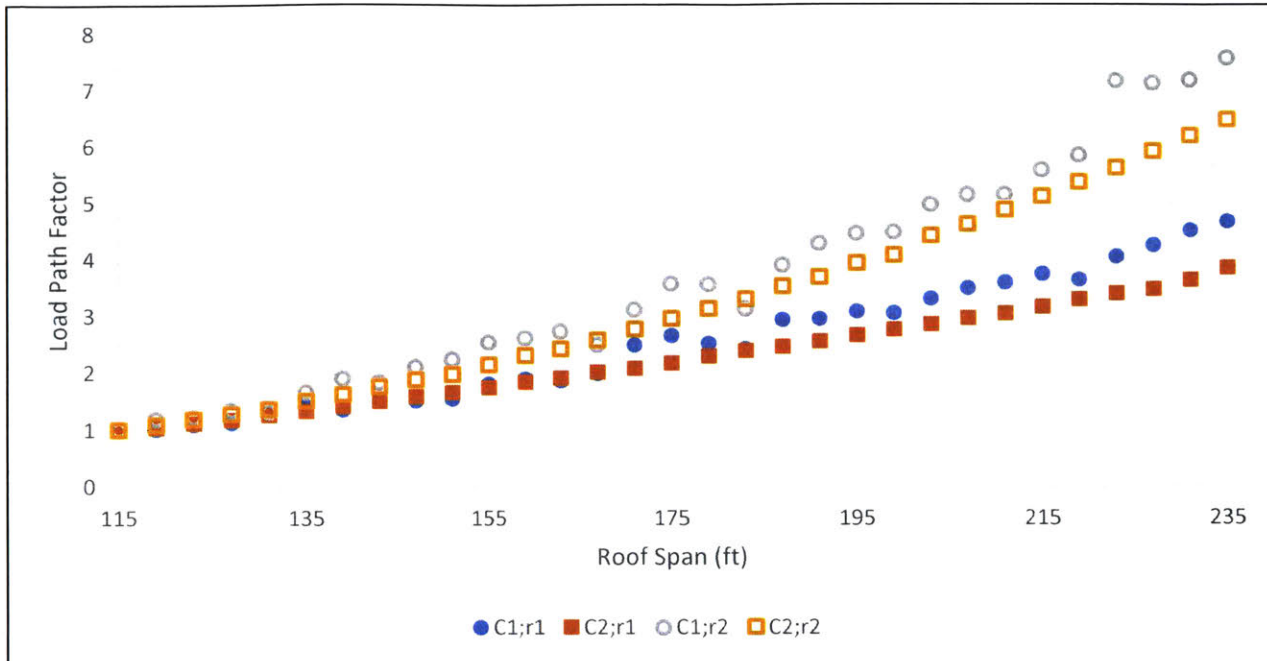


Figure 23. Load Path Factor for circular roof Configurations C1 and C2 when inner ( $r_1$ ) and outer ( $r_2$ ) radii are varied

Figure 23 shows that a larger roof span results in a bigger load path factor and affects the structural efficiency negatively. This result can be understood intuitively, as the increase of the roof span physically increases the load path, and larger load path indicates that the external loads travel more through the structure to get to the foundation and the structure gets more inefficient. Both configurations are similarly influenced by the roof span, with C2 being approximately 10 % more influenced by the roof span than C1.

Figure 23 demonstrates that the influence of the change of the outer ring radius ( $r_2$ ) on the load path factor is greater than that of the inner ring radius ( $r_1$ ). Meanwhile, Figure 24 shows that the total length increases at a similar rate when  $r_1$  or  $r_2$  is changing. “Total length factor” in Figure 24 is the total element length, or the sum of the lengths of all the elements of the structure, divided first by the total roof area and second by the base value in the dataset. As explained before, the load path is calculated through Equations 10 and 11 or  $lp_i = (1/\sigma)\sum|P|L$ . Accordingly, the results showing that  $lp_i$  changes greater when  $r_2$  is varying than when  $r_1$  is varying as Figure 23 shows, and the rates that  $L$  is changing are similar for both cases as Figure 24 shows, indicate that the rate  $|P|$  differs is greater when  $r_2$  is varying than when  $r_1$  is varying.

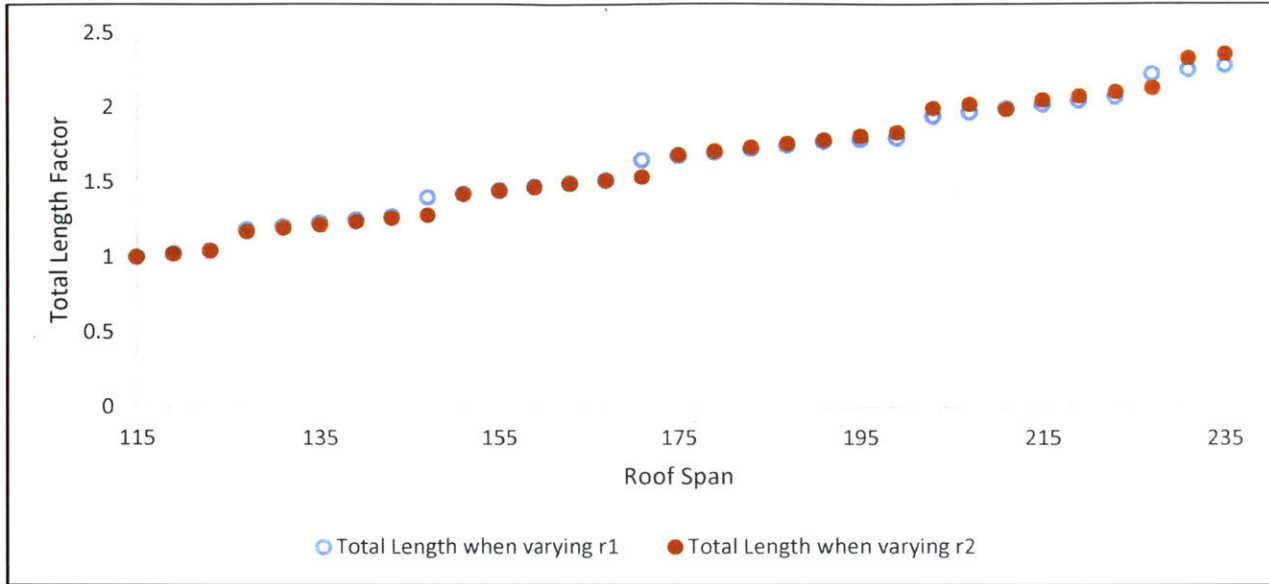


Figure 24. Change in the total length factor with respect to the roof span, when either inner ( $r_1$ ) or outer ( $r_2$ ) radius is varied in the circular roof

Total roof area changes when  $r_1$  and  $r_2$  are varied, respectively, are plotted in Figure 25. Total roof area change is defined as the total roof area normalized by the base value.

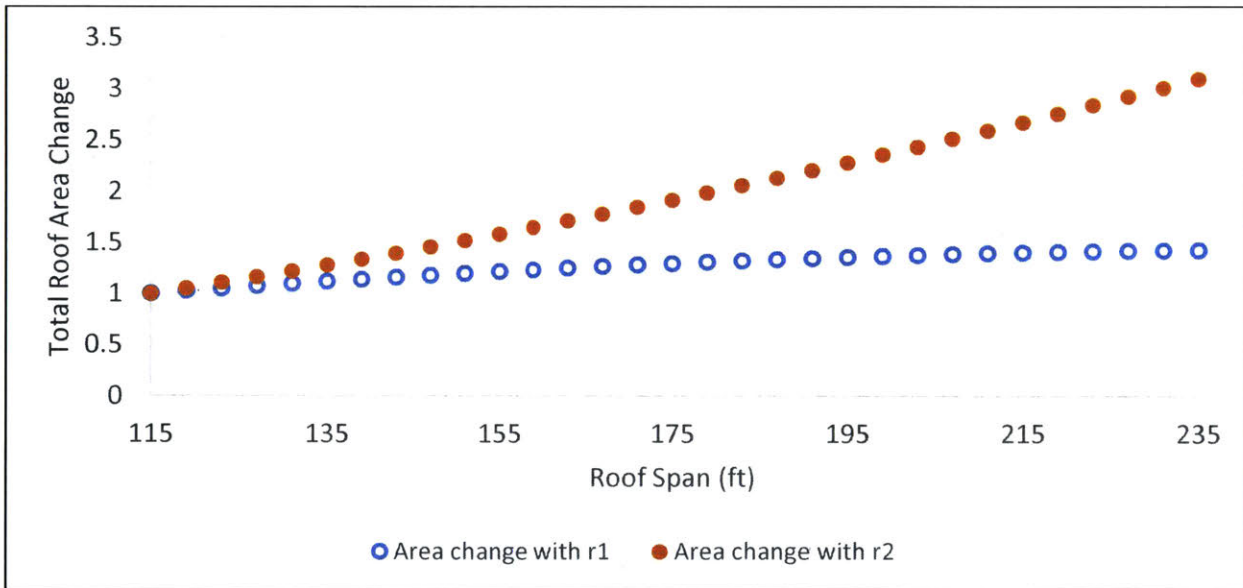


Figure 25. Change in the total circular roof coverage area with respect to the roof span when either inner ( $r_1$ ) or outer ( $r_2$ ) radius is varied

Figure 25 shows that the roof area increases at a faster rate when  $r_2$  is varied than when  $r_1$  is varied. Considering that the load path factor also increases at a faster rate for the same case, the roof area



can be considered to be correlated to the load path factor. By combining results from Figures 23 to 25, it is shown that a larger roof area results in higher axial force including pre-tension and correspondingly, larger load path.

Therefore, the efficiency of a circular spoke wheel roof system increases when its roof span and total size decrease.

### B. Configuration

In order to compare Configurations 1 and 2, total length factor and normalized load path with respect to the roof span when either the inner or outer ring radius changes are plotted in Figure 26. Normalized load path and Normalized total length are used to compare the absolute performance of Configurations 1 and 2. Normalized load path is calculated through Equation 12. Normalized total length is the total element length divided by the total roof area  $A_T$ , and again by the base value. The base value for this case is the total element length of C1 divided by  $A_T$  when the roof span is 115 ft.

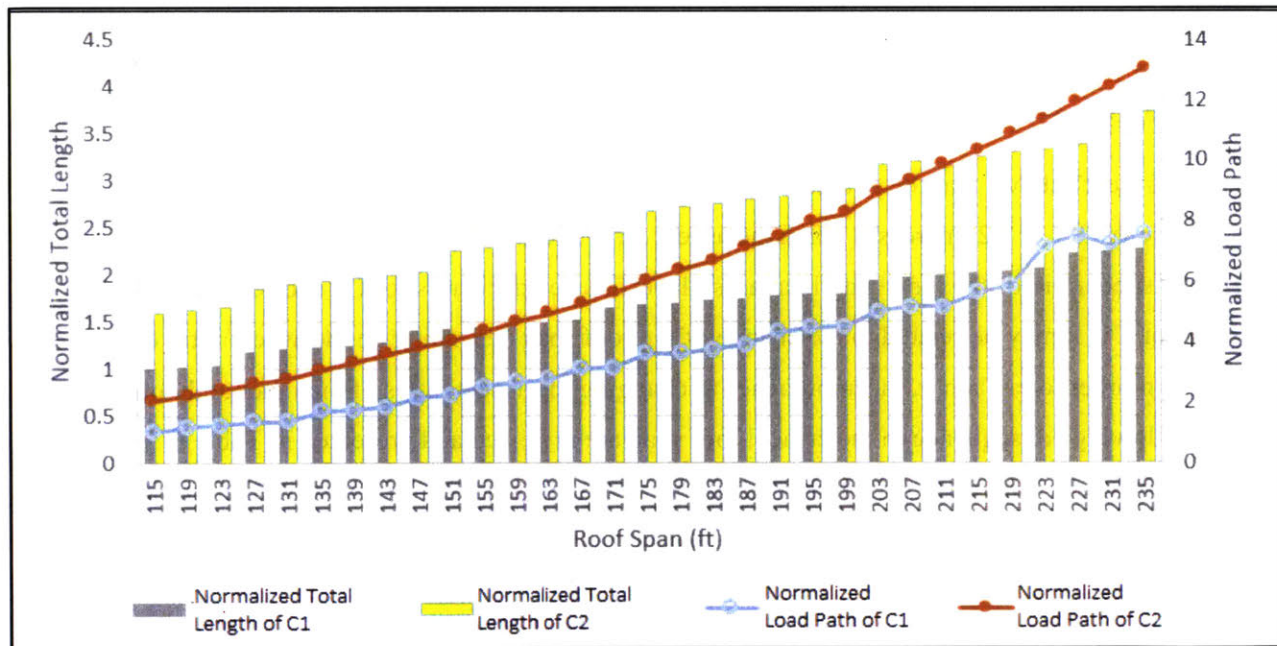


Figure 26. Normalized total element lengths and normalized load path values for Configurations 1 and 2

Figure 26 shows that the both load path factor and normalized total element length for Configuration 2 are about by 50 – 70 % larger than those for Configuration 1 for the same roof span.

Based on Equations 10 and 11 or load path =  $l_{p_i} = (1/\sigma)\sum|P|L$ , these results indicate that the required  $|P|$ , the total axial force including the pre-tension, is similar for Configuration 2 and Configuration 1 for the same roof span. Therefore, Configuration 2 has greater axial forces and accordingly, higher load path or smaller efficiency than Configuration 1.

### C. Aspect Ratio

As noted previously, aspect ratio of a circle or ellipse is defined as the fraction of its radius in the major axis over its radius in the minor axis. In this thesis, first of all, only the aspect ratio of either the inner ring (R(r1)) or the outer ring (R(r2)) is changed while that of the other ring is constant, in order to find out the influence of aspect ratios on the performance. Starting aspect ratios for inner and outer rings are 1 (circle), and the range of the aspect ratio of the varying ring is from 1.00 to 1.70. The variable is represented in the difference in aspect ratio (%), which is calculated as

$$\begin{aligned} & \text{Difference in Aspect Ratio (\%)} \\ &= \left| \frac{(\text{Aspect Ratio of the Varying Ring}) - (\text{Aspect Ratio of the Constant Ring})}{(\text{Aspect Ratio of the Constant Ring})} \right| \end{aligned} \quad (18)$$

Figure 27 shows how much the aspect ratio change of inner or outer rings affects the structural performance of the roof structure, for both configurations.

Figure 27 shows that the structural efficiency of a spoke wheel roof system, whether its configuration is C1 or C2, increases when the aspect ratio of the outer ring increases. On the other hand, when the aspect ratio of the inner ring increases, the efficiency decreases for C2 and remains rather constant for C1. It may be related to the change of the roof span depending on the aspect ratio change of the rings. In order to explain it, the approaches to changing the aspect ratios of the inner and outer rings and the following consequence in the critical roof span are reviewed and presented in Table 6. The “critical roof span” is the span that changes the most within the structure when the aspect ratio of either inner or outer ring changes.

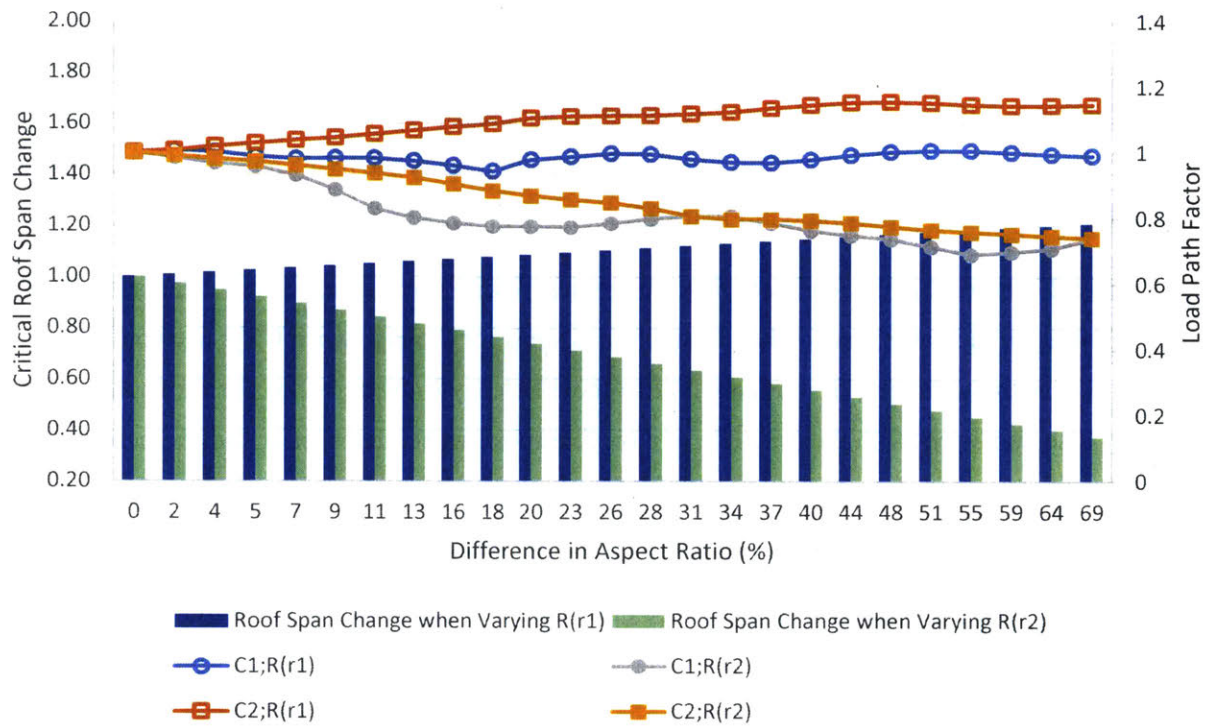


Figure 27. Load path factor and roof span change depending on the aspect ratio change of the inner or outer rings (R(r<sub>1</sub>) or R(r<sub>2</sub>)) and configurations 1 (C1) or 2 (C2)

Table 6. Different approaches of varying the aspect ratio

Aspect Ratio Variation of	Diagram	Critical Roof Span
Inner Ring		Increases
Outer Ring		Decreases

Table 6 shows that the critical roof span, on the side where the inner or outer ring is “compressed” to become elliptical, increases and decreases when the aspect ratio changes for the inner and outer rings, respectively. To validate the assumption that the roof span affects the efficiency, the “critical roof span change,” defined as the critical roof span divided by the base value, is also plotted with respect to the difference in aspect ratio in Figure 27.

Figure 27 shows that the load path factor increases, or the structural efficiency decreases, when the critical roof span increases, except that this pattern is weak for the case when C1 is used and  $r_1$  is varied. It agrees with the finding from Figure 24 that the efficiency is greater when the roof span is smaller. It is also consistent with the principle of a bicycle spoke wheel that shorter spokes increase (radial) stiffness of the wheel, as discussed in Section 1.B.a.

From the discussions above, it is concluded that when the aspect ratio of either inner or outer ring varies, the critical roof span, rather than difference of the aspect ratios of the inner and outer rings, governs the structural efficiency.

Secondly, the aspect ratios of the both inner ( $R(r_1)$ ) and outer ( $R(r_2)$ ) rings are also varied by the same amount. The aspect ratio of both of the rings,  $R$ , where  $R = R(r_1) = R(r_2)$ , and the corresponding load path factors are plotted in Figure 28. The base case for normalization is when the aspect ratio is 1. The variable is represented in terms of the aspect ratio, as it is the same for both inner and outer rings.

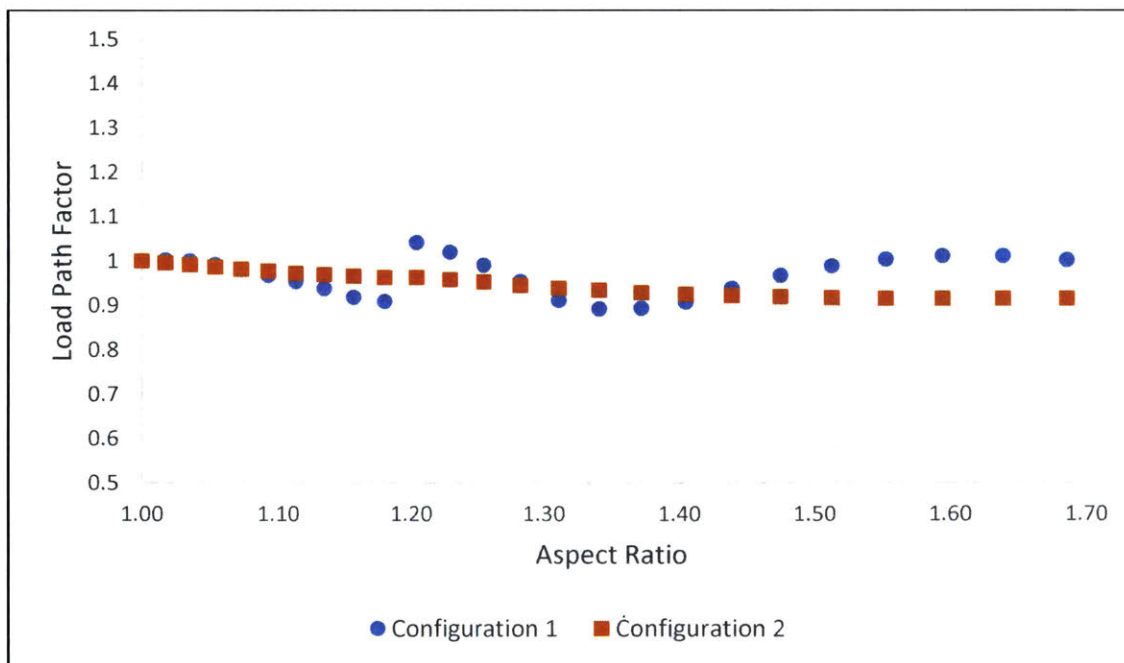


Figure 28. Load Path Factor when both the inner and outer rings have the same aspect ratio  $R$

Figure 28 illustrates that the load path factor remains rather constant when the aspect ratios of the inner and outer ring change at the same rate. When the aspect ratios of both of the rings change concurrently, the critical roof span is constant throughout all the cases with different variable values. Minimal influence of the same aspect ratio changes for both of the rings on the structural efficiency again supports the assumption that the roof span governs the efficiency, rather than the aspect ratio of the rings. It is also consistent with the finding of Bergermann and Göppert (2000) that making the shape of inner and outer rings more elliptical does not greatly disturb the load path and result in significant problems, as long as both rings have the same curvature at each point, as discussed in Section 1.B.b.iii.

#### D. Spoke Spacing and Slope

Spoke spacing in angle is varied and its influence is explored. The number of the spokes ranges from 10 to 32, and correspondingly, the spacing of the spokes ranges from 11 to 33 degrees. Different spoke spacing values and the corresponding load path factors are plotted in Figure 29.

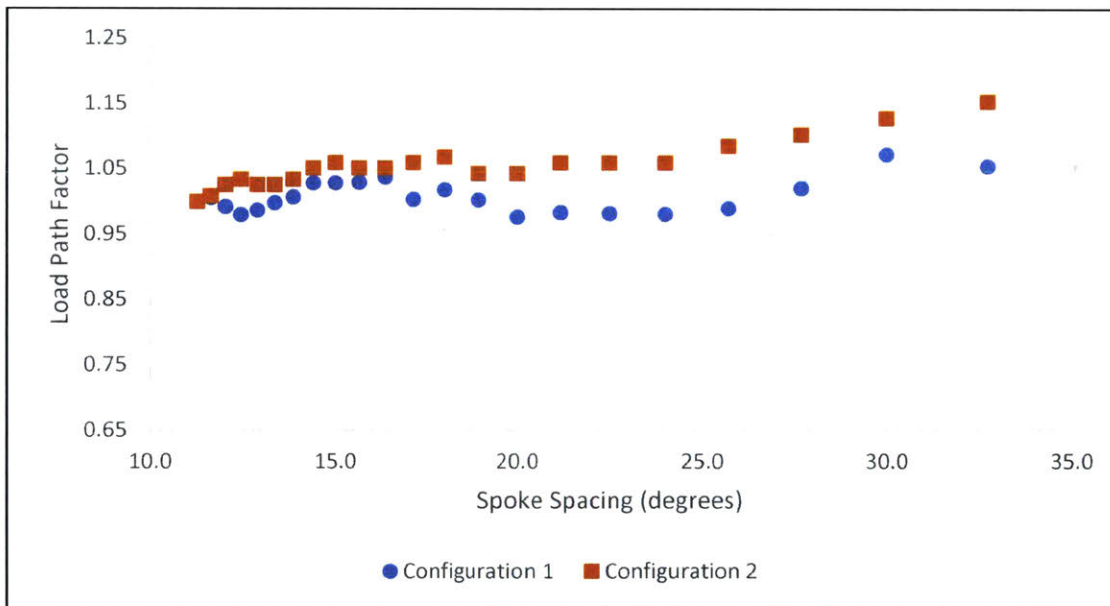


Figure 29. Load Path Factor when spoke spacing ( $\alpha$ ) is varied

Figure 29 shows that the smaller spacing of spokes results in higher performance, though the correlation is not strong. The pattern is valid for both of the configurations, and it agrees with the principle of a spoke wheel system, of which the radial stiffness increases with higher number of spokes.

Spoke slope is varied from 5 to 14 degrees and its effect on the performance is explored as shown in Figure 30.

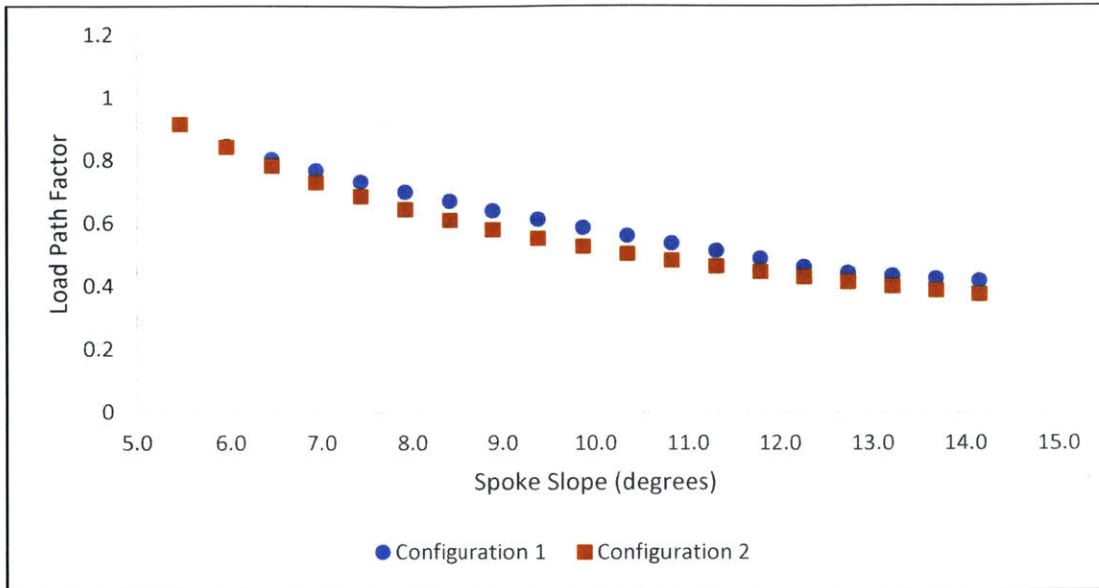


Figure 30. Load Path Factor when spoke slope ( $\theta$ ) is varied

It is clear that a bigger spoke slope yields smaller load path factor or higher structural efficiency for both configurations. It may be because the larger spoke slope provides more structural depth to the system, resulting in smaller force in each member. Although the length of the sloped member increases with the bigger spoke slope, the reduction rate of its inner force turns out to dominate increase rate of its length.

The relationships between the variables and the objective discussed in this section are summarized in the next chapter.

## 4. Conclusion

This thesis explored the history and behaviors of a spoke wheel roof system. In order to determine the influence of geometric variables on the structural performance of the structure, parametric modelling was implemented in Rhinoceros-Grasshopper-Karamba, which resulted in the following findings:

- Governing load case is when the full wind loads are applied, in particular involving internal suction of the roof.
- The decision between Configuration 1 (double tension rings + single compression ring) and Configuration 2 (single tension ring + double compression rings) may depend on architectural needs and location.
  - o In this thesis, assuming that the model is in New York City, USA, Configuration 1 has smaller axial loads and is more efficient than Configuration 2.
- Structural efficiency is greater when the roof span is smaller.
- Structural efficiency is greater when the size of the roof is smaller.
- Roof span has a bigger influence on the structural efficiency than the aspect ratio, when the aspect ratio of either the inner or outer ring varies.
- Varying the aspect ratios of both rings at the same rate does not significantly affect the structural efficiency.
- Decreasing the spoke spacing of spokes increases the efficiency, although the effect is minimal.
- Increasing the spoke slope increases the efficiency.

### **Future work**

The model used in this thesis does not include the columns and their support conditions to the ground, which can affect the structural performance greatly. Also, the Literature Review section notes that the performance decreases when the shape of the rim has straight edges. Therefore, future work is encouraged to explore the following variables and their influence: column height, column support conditions, and rounded rectangle-shaped rims.

Moreover, the effects of different material and section properties for each member may be examined. In particular, using concrete or allowing bending for the compression rings as in many of the existing projects may yield interesting results. The corresponding embodied carbon value considering each material may be another evaluation criterion for the performance.

Applying different climate and the corresponding wind loads to a spoke wheel roof system may show which geometric settings lead to the most efficient structure in each climate condition. Moreover, the region with a significant diurnal or annual temperature change may make the cables more vulnerable to elongation or shortening and going slack, requiring higher pre-tensioning force of the cables. Therefore, accounting for the influence of the temperature change on the cable pre-tension force and relating it to each climatic location shall be considered.

As pre-tension significantly contributes to the project cost and requires special equipment and experience, the structure which requires a lot of pre-tension may not be an optimal case. Therefore, the project cost or constructability may be considered as an evaluation criterion.

Graphic statics may be used to explain the behaviors of a spoke wheel roof system depending on its geometry. Graphic statics is a powerful analysis tool which determines bar forces within a structure solely based on its geometry, by relating a form diagram to its force diagram (Allen & Zalewski, 2010). While its application is limited to determinate structures with only axial forces, as it cannot represent relative stiffness of elements and bending, it may be used for a spoke wheel roof system, which consists mostly of axial members. However, the ability of graphic statics to account for pre-stress is limited, so it may be applicable only to a non-pre-tensioned structure.



## References

- Aghayere, A. & Vigil, J. (2009). *Structural steel design: A practice-oriented approach*. Upper saddle river, NJ: Pearson Prentice Hall.
- American Society of Civil Engineers. (2010). *Minimum Design Loads for Buildings and Other Structures*. Reston, VA: American Society of Civil Engineers.
- Allen E. & Zalewski, W. (2010). *Form and forces: Designing efficient, expressive structures*. NJ: John Wiley & Sons.
- Baker, W.F., Beghini, L.L., Mazurek, A., Carrion, J., & Beghini, A. (2013). Maxwell's reciprocal diagrams and discrete Michell frames. *Structural and Multidisciplinary Optimization*, 48, 267–277
- Bergermann, R. & Göppert, K. (2000). Das Speichenrad - Ein konstruktionsprinzip für weitgespannte dachkonstruktionen. *Stahlbau* 69.8, 595-604.
- Boom, I. (2012). *Tensile-compression ring: A study for football stadia roof structures* (Master's thesis). Retrieved from the TU Delft Repository.
- Brandt, J. (2003). *The bicycle wheel*. Palo Alto, CA: Avocet.
- Building with steel. (1968). [Diagram of structural and architectural systems]. Retrieved from <http://www.newsteelconstruction.com/wp/40-year-ago-americas-largest-cable-suspension-roof-madison-square-gardens-new-york-city/>
- Ghisbain, P. (2013). *1.571: Modeling and analysis of structures Lecture notes*. [PDF document]. Retrieved from stellar.mit.edu
- Holgate, A. (1997). *The art of structural engineering: the work of Jörg Schlaich and his team*. Stuttgart : Edition Axel Menges.
- Krishna, P. (1978). *Cable-suspended roofs*. New York, NY: McGraw-Hill.
- Masubuchi, M. (2013). *Conceptual and structural design of adaptive membrane structures with spoked wheel principle - folding to the perimeter* (Master's thesis). Retrieved from the TU-Berlin Database.
- Mazurek, A., Baker, W.F., & Tort, C. (2010). Geometrical aspects of optimum truss like structures. *Structural and Multidisciplinary Optimization*, 43(2), 231–242.
- Michell, A.G.M. (1904). The limits of economy of material in frame structures. *Philosophical Magazine Series*, 8(47), 589–597
- Prager, W. (1970). Survey paper: Optimization of Structural Design. *Journal of Optimization Theory and Applications*, 6(1).
- Preisinger, C. (2016) *Karamba user manual for version 1.2.2*. [PDF document]. Retrieved from <http://www.karamba3d.com/downloads/>

Schlaich Bergermann Partner. (n.d.). *Projects*. Retrieved from <http://www.sbp.de/en/project/>

Schlaich, J. (2000). Lightweight Structures. In M. Barnes & M. Dickson, *Widespan Roof Structures* (pp. 178 - 188). Reston, VA: Thomas Telford Publishing

Stromberg, L.L., Beghini, A., Baker, W.F., & Paulino, G.H. (2012). Topology optimization for braced frames: combining continuum and beam/column elements. *Engineering Structures*, 37,106–124.

The New York City Department of Buildings. (2014). *2014 New York City Construction Codes*. New York, NY: The New York City Department of Buildings.